สมบัติการดูดซับของยางธรรมชาติเติมด้วยวัสดุซิลิกา

นางสาวปาริชาต กล่ำรัศมี

วิทยานิพนธ์นี้เป็นส่วนหนึ่งของการศึกษาตามหลักสูตรปริญญาวิทยาศาสตรมหาบัณฑิต
สาขาวิชาวิชาปิโตรเคมีและวิทยาศาสตร์พอลิเมอร์
คณะวิทยาศาสตร์ จุฬาลงกรณ์มหาวิทยาลัย

ปีการศึกษา 2551

ADSORPTION PROPERTIES OF NATURAL RUBBER FILLED
WITH SILICA MATERIALS
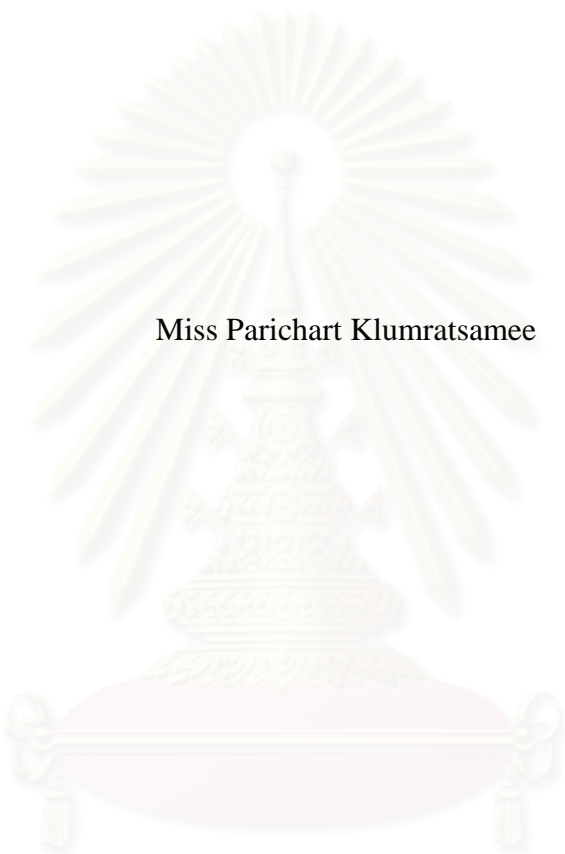
Miss Parichart Klumratsamee

A Thesis Submitted in Partial Fulfillment of the Requirements
for the Degree of Master of Science Program in Petrochemistry and Polymer Science
Faculty of Science
Chulalongkorn University
Academic Year 2008

Thesis Title	ADSORPTION PROPERTIES OF NATURAL RUBBER FILLED WITH SILICA MATERIALS
By	Miss Parichart Klumratsamee
Field of Study	Petrochemistry and Polymer Science
Advisor	Assistant Professor Chawalit Ngamcharussrivichai, Ph.D.
Co-Advisor	Sirilux Poompradub, Ph.D.

Accepted by the Faculty of Science, Chulalongkorn University in Partial Fulfillment of the Requirements for the Master's Degree

.... Dean of the Faculty of Science

(Professor Supot Hannongbua, Dr.rer.nat)

THESIS COMMITTEE

.... Chairman

(Professor Pattarapan Prasassarakich, Ph.D.)

.... Advisor

(Assistant Professor Chawalit Ngamcharussrivichai, Ph.D.)

.... Co-Advisor

(Sirilux Poompradub, Ph.D.)

.... Examiner

(Associate Professor Wimonrat Trakarnpruk, Ph.D.)

.... External Examiner

(Assistant Professor Warunee Ariyawiriyanan, Ph.D.)

ปาริชาต กล่ำรัศมี : สมบัติการดูดซับของยางธรรมชาติเติมด้วยวัสดุซิลิกา. (ADSORPTION PROPERTIES OF NATURAL RUBBER FILLED WITH SILICA MATERIALS) อ. ที่ปรึกษาวิทยานิพนธ์หลัก : ผศ.ดร. ชวลิต งามจรัสศรีวิชัย อ. ที่ปรึกษาร่วม : ดร.ศิริลักษณ์ พุ่มประดับ, 96 หน้า

งานวิจัยนี้ศึกษาวิธีการเตรียมคอมพอสิตของยางธรรมชาติกับวัสดุซิลิกาชนิดต่างๆ เพื่อให้ได้คอมพอสิตที่มีพื้นที่ผิวสูง และมีสมบัติการดูดซับ วัสดุซิลิกาที่ใช้ได้แก่ ซิลิกาเจลที่มีขนาด อนุภาคต่าง ๆ กัน และเมโซพอรัสซิลิกา (mesoporous silica) เช่น MCM-41 และ SBA-15 อิทธิพล ของปัจจัยต่างๆที่มีผลต่อการกระจายตัวของวัสดุซิลิกาในยางธรรมชาติและความพรุนของคอมพอสิต ได้แก่ การปรับเปลี่ยนหมู่ฟังก์ชันบนพื้นผิวของวัสดุซิลิกาเพื่อเพิ่มความเข้ากันได้ระหว่างยางธรรมชาติ กับวัสดุซิลิกา วิธีการเตรียมคอมพอสิต ชนิด ปริมาณ และขนาดอนุภาคของวัสดุซิลิกา และการเผาเม โซพอรัส ซิลิกาถูกศึกษา การศึกษาชี้ให้เห็นว่าความพรุนของคอมพอสิตเพิ่มขึ้นเมื่อเพิ่มปริมาณและ ลดขนาดอนุภาคของวัสดุซิลิกา ยิ่งไปกว่านั้นการปรับเปลี่ยนหมู่ฟังก์ชันบนพื้นผิวของวัสดุซิลิกาแทบ ไม่มีผลต่อการกระจายตัวของวัสดุซิลิกาในคอมพอสิต แต่ส่งผลให้ความพรุนของคอมพอสิตที่ ประกอบด้วยวัสดุซิลิกาซึ่งผ่านการปรับเปลี่ยนหมู่ฟังก์ชันมีค่าลดลง นอกจากนั้นวิธีการกวนผสมแบบ แขวนลอย (slurry technique) เป็นวิธีการที่เหมาะสมในการเตรียมคอมพอสิตที่มีความพรุนสูง เมื่อ วัสดุซิลิกามีปริมาณเพิ่มขึ้น หรือมีขนาดอนุภาคเล็กลง ทำให้ความพรุน ของคอมพอสิตมีค่าสูงขึ้น ที่ ปริมาณวัสดุซิลิกาเท่ากัน คอมพอสิตที่เตรียมจาก MCM-41 จะมีความพรุนมากที่สุด จากการศึกษา การดูดซับและการคายดูดซับวิตามินซีของคอมพอสิต ชี้ให้เห็นว่าปริมาณการดูดซับและการคายดูด ซับของคอมพอสิตที่ประกอบด้วยซิลิกาเจลเพิ่มขึ้นเมื่อพื้นที่ผิวจำเพาะ (S_{BET}) และปริมาตรรูพรุนเฉลี่ย (V_p) ของคอมพอสิตมีค่าสูงขึ้น แต่ปริมาณการดูดซับและการคายดูดซับของคอมพอสิตที่ประกอบด้วย เมโซพอรัส ซิลิกาขึ้นอยู่กับขนาดของรูพรุนระหว่างอนุภาค (interparticle voids) บนพื้นผิวของคอม พอสิต

ลาขาวิชา...ปิโตรเคมีและวิทยาศาสตร์พอลิเมอร์...ลายมือชื่อนิสิต...ปาริชาต กล่ำรัศมี...

ปีการศึกษา......2551.................................ลายมือชื่อ อ. ที่ปรึกษาวิทยานิพนธ์หลัก...............

ลายมือชื่อ อ. ที่ปรึกษาวิทยานิพนธ์ร่วม...............

497 23745 23   : MAJOR PETROCHEMISTRY AND POLYMER SCIENCE

KEYWORDS: NATURAL RUBBER / SILICA MATERIAL/ SILYLATION / ADSORPTION / ASCORBIC ACID

PARICHART KLUMRATSAMEE: ADSORPTION PROPERTIES OF NATURAL RUBBER FILLED WITH SILICA MATERIALS. ADVISOR: ASSISTANT PROFESSOR CHAWALIT NGAMCHARUSSRIVICHAI, Ph.D., CO-ADVISOR: SIRILUX POOMPRADUB, Ph.D., 96 pp.

The present research has studied the preparation of composite from natural rubber (NR) and various silica materials with high surface area and adsorption property. The silica materials include silica gel with various particle sizes and mesoporous silicas, i.e., MCM-41 and SBA-15. Influences of several parameters that affect dispersion of silica particles in NR and porosity of composite such as surface modification of silica materials to increase compatibility between NR and silica materials, preparation of NR composite, types, contents and sizes of silica materials, and calcination of mesoporous silicas were studied. The studies indicated that porosity of resulting NR composite increased with increasing content and decreasing size of silica material. Moreover, surface modification of silica materials hardly affects dispersion of silica particles in NR. However, it resulted in decreasing porosity of NR composite consisted functionalized silica materials. Further, slurry technique was appropriate preparation of NR composite with high porosity. With either increasing the silica content or decreasing the silica particles, porosity of the NR composites were increased. At equal loading of silica material, NR composite consisted of MCM-41 has highest porosity. From the study of vitamin C adsorption and desorption of NR composite, it indicated that adsorption and desorption quantity of NR composite filled with silica gel increased with increasing BET surface area and average pore volume of NR composite; while, one of composite filled with mesoporous silicas depended on size of interparticle voids on surface of composite.

Field of Study: Petrochemistry and Polymer Science..Student's Signature. Parichart Klumratsamee

Academic Year:...2008...............................Advisor's Signature Chawalit N. ....

Co-Advisor's Signature... Sirilux P...

ACKNOWLEDGEMENTS

CONTENTS

LIST OF TABLES

LIST OF FIGURES

LIST OF SCHEMES

LIST OF ABBREVIATIONS

AA	: Ascorbic Acid
Å	: Angstrom
°C	: Degree Celsius
cm	: Centimeter
cal	: Calorie
cc	: Cubic Centimeter
g	: Gram
h	: Hour
IUPAC	: International Union of Pure and Applied Chemistry
kJ	: Kilojoule
L	: Liter
M	: Molar
mm	: Millimeter
mol	: Mole
mL	: Milliliter
NR	: Natural Rubber
nm	: Nanometer
P/P_0	: Relative Pressure
Phr	: Part Per Hundred Part of Rubber
pK_a	: Acid Dissociation Constant
psi	: pound per square inch
R^2	: Coefficient of Determination
M	: Molar
STP	: Standard Temperature and Pressure
sec	: Second
V	: Volt
wt.%	: Weight Percentage
% w/v	: Weight -volume Percentage
µm	: Micrometer
µg	: Microgram

λ_{max} : Highest Wavelength Value

ε_{max} : Highest Transmittance Value

2θ : Two-theta Angle

CHAPTER I

INTRODUCTION

1.1 The Statement of Problem

Natural rubber (NR) can be used as the host polymer to produce several products because of good flexibility, easily to process, low density and good chemical resistance. In addition, NR is abundantly available in Southeast Asia and not expensive. However, NR has some disadvantages when compare with synthetic rubber (Morton, 1973). Adsorption property of NR was limited only hydrophobic materials. Therefore, the application and development of a new material is required to increase advantage and value of product. So, NR is usually added the additives to improve its properties.

Silica materials are general kind of additives to enhance NR properties. It is known to have high thermal stability and surface area, which results in high surface capacity for adsorption. Silica particles contain unreacted silanols and siloxanes. Silanols are considered to be adsorption sites for hydrophilic molecule. Therefore, silica materials are excellent polar adsorbents. Then silica materials have been applied to blend with NR such as silica gel and mesoporous silicas (e.g. MCM-41 and SBA-15). Ordinarily, NR is hydrophobic matrix part and silica material is hydrophilic reinforcing part.

To prevent phase separation between the hydrophilic and hydrophobic parts, silylation is reaction to functionalize silica material surface using different organosilanes such as trimethylchlorosilane and propyltrimethoxysilane that can increase hydrophobic structure in silica material to improve compatibility between two parts.

This thesis concerns to preparation of NR composite with high adsorption capability that preparation method is investigated. Additionally, the effect of type, size, content, calcination, and functionalization of silica material on porosity of resulting composite are studied. The NR composite will be useful for adsorption of polar material as ascorbic acid from aqueous solution. Therefore, ascorbic acid adsorption and desorption of prepared NR composite are also studied. Furthermore, the influence of ahead mention on ascorbic acid adsorption and desorption capability of resulting composite is also observed. Moreover, adsorption and desorption capability of NR composite after vulcanization to enhance stability is investigated.

1.2 Objective of the Research Work

The objective of this research is to prepare NR composite with high surface area and ascorbic acid adsorption and desorption capability.

1.3 Scope of the Research Work

The experimental procedures are carried out as follows:

1. Survey literature and study the research work.
2. Synthesize mesoporous silica (MCM-41 and SBA-15) and sieve silica gel as 149-210 (Si1), 99-149 (Si2), 74-99 (Si3), and 63-74 (Si4) μm.
3. Modify functional group of silica material by silylation technique.
4. Investigate carbon and hydrogen content in structure of funtionalized silica material using CHN analyzer.
5. Prepare the NR composite filled silica material 100-300 phr by two-roll mill and slurry technique.
6. Investigate the silica particles distribution in NR composite using scanning electron microscope.
7. Investigate the textural properties of NR composite using surface area and porosity analyzer.

8. Investigate the adsorption properties of NR composite using UV/Vis spectrophotometer.

9. Summarize the results.

CHAPTER II

THEORY AND LITERATURE REVIEWS

2.1 Natural Rubber

Natural Rubber (NR) can be isolated from more than a thousand different species of plan, the Para rubber tree (*Hevea brasiliensis*), is practically the sole source of commercial rubber today. By the end of eighteens centuries, Europe and America were using a few tons of rubber per year. However users found it difficult to work with solid rubber. Moreover, articles make from NR turned sticky in hot weather and stiffened in the cold. In 1820, Thomson Hancock invented a machine called "masticator" that allow solid rubber to be softened (Morton, 1973). The British considered the possibility of cultivating rubber in Asia. The rubber tree arrived in Sri Lanka in 1876 and Malaysia the following year. In 1880 *Hevea* seeding were widely distributed in Asia. The land used for rubber cultivation and the production of NR has grown steadily as expected since World War II (Morton, 1973). Thailand was the biggest producer, followed by Indonesia and Malaysia. The world production of NR is shown in Table 2.1.

Table 2.1 World production of NR (2001-2007) (Thai Rubber Association, 2008)

unit: 10^3 tons

Year	Thailand	Indonesia	Malaysia	India	Vietnam	China	Sri Lanka	Brazil	Cambodia	world grand total
2001	2319.5	1607.3	782.6	631.5	312.6	478.0	86.2	88.1	42.0	7328
2002	2615.1	1630.0	804.9	640.8	331.4	527.0	90.5	89.0	43.0	7332
2003	2876.0	1792.2	909.2	707.1	363.5	565.0	92.0	94.0	45.0	8033
2004	2984.3	2066.2	1097.5	742.6	419.0	573.0	94.7	101.4	43.0	8748
2005	2937.2	2271.0	1060.7	771.5	468.6	510.0	104.4	106.5	44.5	8882
2006	3137.0	2637.0	1284.0	853.3	553.5	533.0	109.2	108.3	64.0	9680
2007	3056.0	2791.0	1215.0	767.0	608.0	577.0	120.0	111.0	68.0	9685

2.1.1 Physical Properties

Physical properties of NR may vary slightly due to the non-rubber constituents present and to the degree of crystallinity. When NR is held below 10 $^\circ$C, crystallization occurs, resulting in a change of density from 0.92 to about 0.95 (Brydson, 1978). Listed in Table 2.2 are some average physical properties.

Table 2.2 Physical Properties of NR

Properties	value
Density	0.92 g/cm^3
refractive index (20 $^\circ$C)	1.52
coefficient of cubical expansion	0.00062 /$^\circ$C
cohesive energy density	63.7 cal/cc.
heat of combustion	10,700 cal/g
thermal conductivity	0.00032 cal/sec/cm^3/$^\circ$C
dielectric constant	2.37
power factor (1,000 cycles)	0.15-0.2*
volume resistivity	10^{15} ohms/cc.
dielectric strength	1,000 V/mm

* The power factor is reduced to 0.0015 and the resistivity substantially increased in deproteinized rubber.

2.1.2 Composition and Structure of NR

The empirical for the NR molecule appears to have been first determined by Faraday who reported his finding in 1826. He concluded that carbon and hydrogen were the only elements present and his results correspond to the formula C_5H_8 (Morton, 1973).

The fundamental structure of NR was firstly found to have the formula C_5H_8, so-called isoprene, for which Tilden proposed the structure as Figure 2.1 (Morton, 1973).
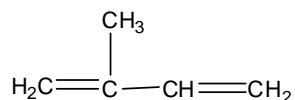
Figure 2.1 Isoprene structure.
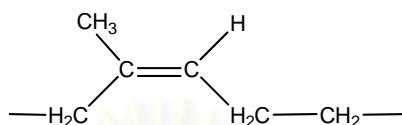
Figure 2.2 Cis-repeating unit**.**
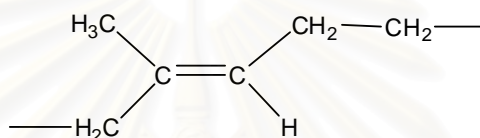
Figure 2.3 Trans-repeating unit.

The linear structures of isoprene were proposed by Pickles, providing for the structure isomerism with both *cis-* and *trans-* repeating units as shown in Figure 2.2 and 2.3, respectively (Morton, 1973).

It is known that these are the major hydrocarbon components of *Hevea brasiliensis* used for belting, submarine cable, golf ball and container applications. For the structural studies, the earlier work could suggest that NR was *trans*-polymer; however, later studies of X-ray fiber diagrams of stretched NR revealed that NR was the *cis*-polymer.

The possibility is that NR chain might contain a mixture of *cis-* and *trans*-groups. However, it was considered to be unlikely because such a mixed polymer would have an irregular structure and be unable to crystallize in the manner of NR. Infrared studies have subsequently confirmed that NR was the *cis*-polymer. Moreover, these studies have indeed shown that NR was at least 97% *cis*-1,4-polyisoprene and the other were 1,2-structure and 3,4-structure as shown in Figure 2.4 (Brydson, 1978).

(a)   (b)   (c)
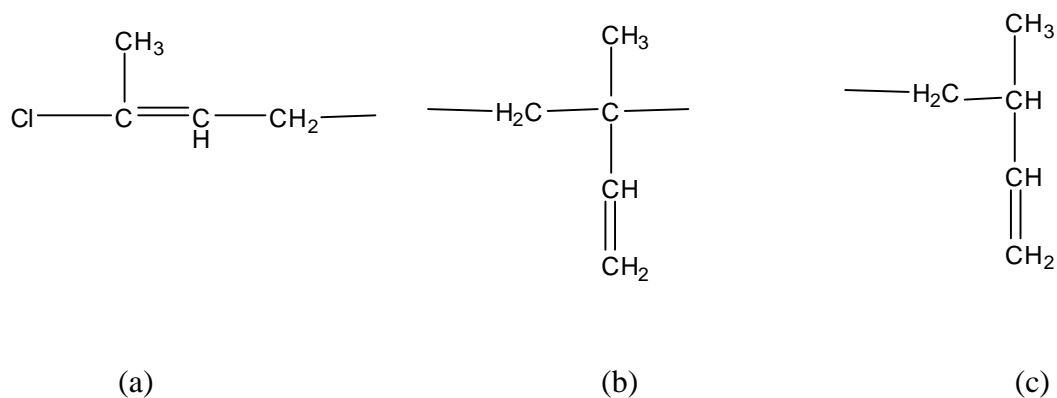
Figure 2.4 Structure of polyisoprene isomer: (a) 1,4-polyisoprene (b) 1,2-
polyisoprene (c) 3,4-polyisoprene.

2.2 Silica Materials

Silica is an inorganic polymer with the general structural formula of $(SiO_2)_n$. Typically, silica can be classified according to IUPAC in three types depending on its pore size.

1. Microporous silica with pore diameter smaller than 2 nm.
2. Mesoporous silica with pore diameter between 2 and 50 nm.
3. Macroporous silica with pore diameter larger than 50 nm.

Silica was usually made by acidification of sodium silicate or polymerization of silicic acid. Also, this material could be synthesized via sol-gel process as written in Equation 2.1-2.3 (Blow, 1980).

Hydrolysis: $-\overset{|}{\underset{|}{Si}}-OR + H_2O \rightleftharpoons -\overset{|}{\underset{|}{Si}}-OH + ROH$ (2.1)

Alcohol condensation: $-\overset{|}{\underset{|}{Si}}-OR + HO-\overset{|}{\underset{|}{Si}}- \rightleftharpoons -\overset{|}{\underset{|}{Si}}-O-\overset{|}{\underset{|}{Si}}- + ROH$ (2.2)

Water condensation: $-\overset{|}{\underset{|}{Si}}-OH + HO-\overset{|}{\underset{|}{Si}}- \rightleftharpoons -\overset{|}{\underset{|}{Si}}-O-\overset{|}{\underset{|}{Si}}- + H_2O$ (2.3)
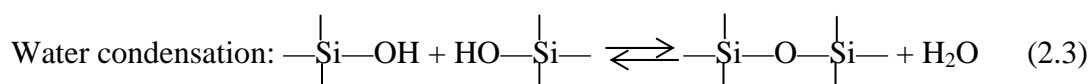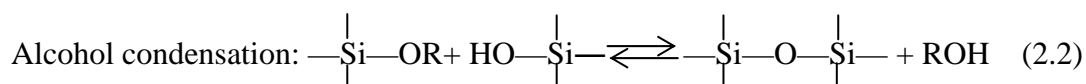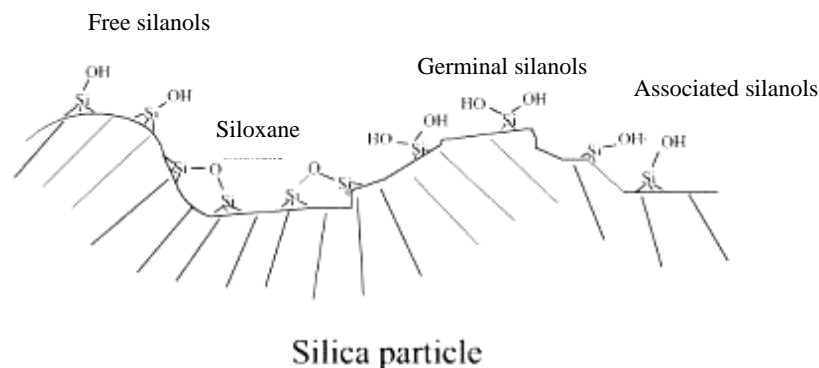
Figure 2.5 Schematic structure of a silica gel showing siloxane bond, free silanols, geminal silanols and associated silanols.

The silica particles contain unreacted silanols and siloxanes. The silanols are considered to be adsorption sites for hydrophilic molecule, while the siloxanes are hydrophobic. The form of silanols on the surface may be single, geminal and vicinal in Figure 2.5.

The silanol groups present on the silica surface have a weak acidic character, which the proton dissociation is displayed as Equation 2.4.

$$\text{Si-OH} \quad \rightleftarrows \quad \text{Si-O}^- + \text{H}^+ \qquad (2.4)$$
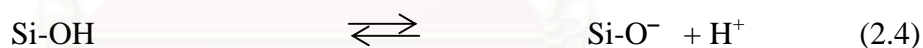
The pKa value of this reaction is about 6.8 ± 0.5 (Blow, 1980).

The dispersion and the distribution of silica are generally recognized to be the state of aggregation and agglomeration, which are schematically shown in Figure 2.6. Aggregates, which are three-dimentional clusters of ultimate particles, can physically agglomerate through intermolecular hydrogen bonding of surface silanol groups of one aggregate to a silanol group of other aggregate as Figure 2.6.

Primary particle   Aggregates   Agglomerate

10 nm – 100 nm   100 nm -1000 nm   1 µm – 1000 µm
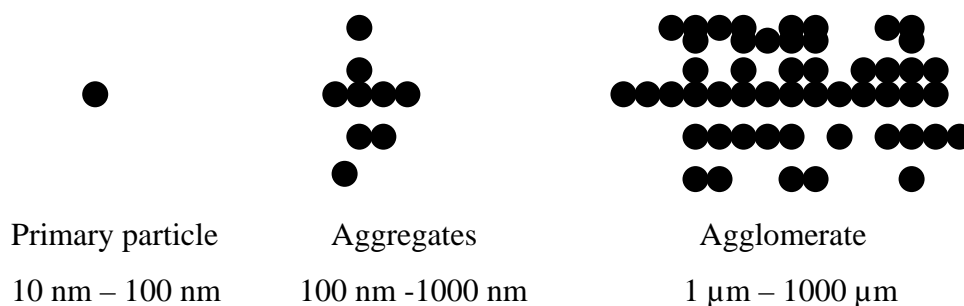
Figure 2.6 Sketches of a primary particle, aggregates and agglomerate occurring in
silica.

2.2.1 Silica Gel

Silica gel, an oxide of the element silicon, is an amorphous and partially
hydrated form of silica; further, porous form of silica was made synthetically from
several production methods. Typically, silica gel can be classified into two types
depending on its synthesis.

2.2.1.1 Hydrated Precipitated Silica

In the case of precipitated silica, the reaction mixture is held in the
alkaline pH region, and offers limited aggregates of primary particles with a diameter
of >5 nm, and specific surface area of <350 m^2/g (Mark *et al.*, 2005). The production
of precipitated silica starts with the reaction of an alkaline silicate solution with a
mineral acid. Sulfuric acid and sodium silicate solutions are added simultaneously to
water under agitation. The resulting white precipitate is filtered, washed and dried in
the manufacturing process. This silica is silicon dioxide containing 10-14% water,
with particle size in the range of 10-40 nm. They are reinforcing fillers giving
compounds of high tensile strength, tear strength and good mechanical abrasion.

2.2.1.2 Fumed Silica or Pyrogenic Silica

One production method for the production of fumed silica involved a continuous flame hydrolysis technique. It involves the conversion of silicon tetrachloride ($SiCl_4$) to the gas phase using an oxy hydrogen flame. It then reacts with water to yield silica (SiO_2) and hydrochloric acid as Equation 2.5.

$$SiCl_4 + H_2O \longrightarrow SiO_2 + HCl \qquad (2.5)$$

HCl is easily separated as it remains in the gas phase, while the fumed silica is solid

Fumed or pyrogenic silica is silicon dioxide, containing less than 2% combined water. The silica with very small particle size is highly reinforcing fillers, given high tensile strength, tear resistance, abrasion resistance.

2.2.2 Mesoporous Silica

Periodic mesoporous silica had been discovered in 1990, or even much earlier, this type of materials did not attract much attention until 1992, upon the publication of two groundbreaking papers by a group of Mobil's scientists describing the so-called M41S family of mesoporous silicas. Since then, research in this topic has grown so dramatically that it has developed into a separate field. The M41S silicas consist of three mesophases, namely MCM-41 with hexagonal structure, MCM-48 with cubic structure and MCM-50 with lamella structure. They are synthesized via a supramolecular templating mechanism using long chain alkyltrimethylammonium surfactants under basic conditions. FSM-16, HMS and SBA-15 are the mesoporous silica with a similar structure to MCM-41 (Yang, 2003). Currently, periodic mesoporous silicas may be readily prepared under an extremely wide range of conditions. Figure 2.7 shows schematically the structural parameters that have been explored in design and synthesis of periodic mesoporous silicas. The mesoporous silicas, which were studied in this research, are MCM-41 and SBA-15.

Pore System   Internal Surface

 - size   - functionalization

 - shape   - hydrophobicity

 - connectivity

 - structure

Pore Walls   Particles

 - composition   - morphology

 - thickness   - orientation

 - cystallinity

 - stability (hydrothermal, mechanical)
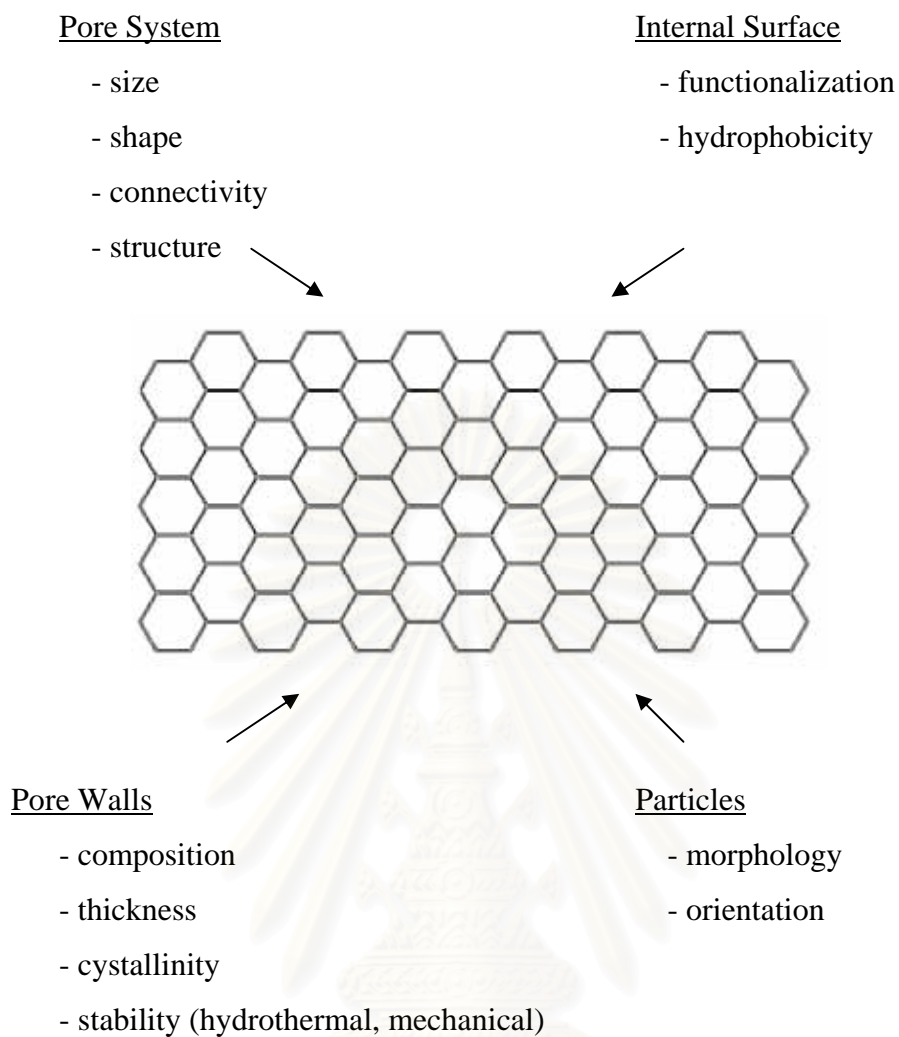
Figure 2.7 Structural parameters for the design of nanostructured materials (Yang, 2003).

2.2.2.1 MCM-41

MCM-41 (Mobil Crystalline of Materials) composes of amorphous silica, it displays an ordered structure with uniform mesopores arranged into a hexagonal, honeycomb-like lattice. In Figure 2.8 shows directly inside the uniform mesopores, which are separated from each other by thin walls of amorphous silica, approximately 1 - 1.5 nm thickness. The mesopores are not necessarily running in a straight way through the silica matrix, but they can be slightly curved, thereby retaining the hexagonal ordering. MCM-41 has a very large void fraction and a rather low density due to the presence of the mesopores. As a result of MCM-41 displays a very large specific surface area of approximately 1,000 m^2/g. This property makes MCM-41 very interesting to be used as a support material for heterogeneous catalysts.
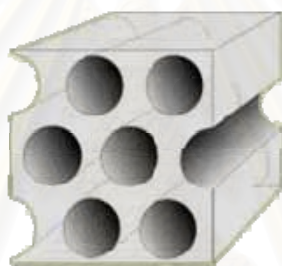
Figure 2.8 Two hexagonal channels of MCM41 (Tyndall National Institue, 2008).

Despite the advantages mentioned above, there is one eminent drawback associated with MCM-type materials, those are a resulting of very thin, amorphous pore walls. Because of very large mesopore surface area, the pore walls are extremely reactive towards mineralizing agents, i.e. hydroxide and fluoride ions, resulting in the collapse of the thin walls upon exposure to these agents; because, these agents dissolve silica. As a result the stability of MCM-41 in aqueous solutions is limited to pH values $\leq$ 7. Moreover, the chemical affinity of the pore surface towards precursors of catalytically active phases sometimes also results in the collapse of the hexagonal framework structure.

2.2.2.2 SBA-15

Researchers at the University of California in Santa Barbara announced the production of silica material with difference pore sizes between 46 to 300 Å. This material processing a hexagonal array of pores is SBA-15.

Hexagonal mesoporous, SBA-15, with large uniform pore size (up to ~ 300 Å) are obtained by using of amphiphilic block copolymer as organic structure-directing agents. Using aqueous acidic conditions and dilute triblock copolymer concentration, SBA-15 has a highly ordered-dimentional hexagonal mesostructure and thick uniform silica walls. The hydrothermal stability of SBA-15 is higher than that of MCM-41 with thinner walls, made with conventional cationic surfactants.

2.3 Silylation

Silylation is a chemical reaction which functionalizes silica materials via surface reaction between an organosilane and silanol group ($\equiv$Si-OH). Organosilane, otherwise known as silane coupling agent, whose structure is R-CH_2-Si-X_3 where R is an alkyl or aryl and X is a methoxy, ethoxy, acetoxy group, or halogen. Trimethylchlorosilane ($(CH_3)_3SiCl$) and hexamethyldisiloxane ($((CH_3)_3Si)_2O$) are organosilanes that can increase hydrophobicity of silica surface. When trimethylchlorosilane is used as functionalizing agent, the reaction is called trimethylsilylation (Koyano *et al.*, 1997). Generally, trimethylsilylation is illustrated in Equation 2.1.

$$\text{sample}\!-\!\text{OH} + \text{CH}_3\!-\!\overset{\overset{\displaystyle \text{CH}_3}{|}}{\underset{\underset{\displaystyle \text{CH}_3}{|}}{\text{Si}}}\!-\!\text{Cl} \longrightarrow \text{sample}\!-\!\text{O}\!-\!\overset{\overset{\displaystyle \text{CH}_3}{|}}{\underset{\underset{\displaystyle \text{CH}_3}{|}}{\text{Si}}}\!-\!\text{CH}_3 + \text{HCl}$$
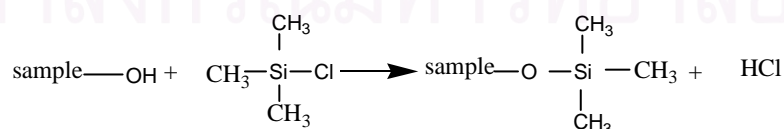
Equation 2.1 Trimethylsilylation chemical equation (Koyano *et al.*, 1997).

Other organosilanes, often used in field of material science include propyltrimethoxysilane (($CH_3O)_3Si(CH_2)_2$-CH_3) (Yokoi *et al.*, 2004) and 3-aminopropyltrimethoxysilane ($NH_2CH_2CH_2CH_2Si(OCH_3)_3$). Propyltrimethoxysilane has longer hydrocarbon chain than trimethylchlorosilane. 3-aminopropyltrimethoxysilane resulted in an increase hydrophilicity of silica surface to provide the surface of silica with high basicity function.

2.4 Composite

The word "composite" in composite material signifies that two or more materials are combined to form a useful material. The advantage of composite is that it usually exhibits the best qualities of its constituents and often some qualities that neither constituent possesses (Jones, 1975). The properties that can be improved by forming a composite material include:

- strength	- fatigue life
- stiffness	- temperature-dependent behavior
- corrosion resistance	- thermal insulation
- wear resistance	- thermal conductivity
- attractiveness	- acoustical insulation
- weight	- adsorption

Commonly, all of the properties above are not improved at the same time. The applications of final product determine that which properties should be improved.

2.4.1 Composition of Composite Materials

2.4.1.1 Matrix

Matrix, that is continuous phase, is a major constituent into which the reinforcement is embedded. It holds reinforcing material together and also determines the physical properties of the end products. In structural applications, the matrix is

usually a light metal such as aluminium or titanium, which is added by fiber glass reinforcing material. The composite obtained is used for automobile part to reduce weight of vehicle. Moreover, the other matrix can be ceramics, polymers, and wood.

2.4.1.2 Reinforcing Materials

The reinforcing materials are embedded into the matrix. They can normally enhance stiffness, strength and sometimes improve toughness. Properties of composite are directly related to their atomic arrangement and their content. The particle reinforcing materials are arranged in matrix as fiber, they can improve strength higher than wide dispersed in composite.

Different shapes of reinforcing materials:

- fiber/filament   - woven

- flake   - needle

- aggregate   - particulate

- globular   - platelet

Reinforcing materials are classified according to their shapes. For example, fiber reinforcing materials and particulate reinforcing materials.

2.4.2 Classification and Characteristics of Composite Materials

There are three commonly accepted types of composite materials:

(A) Fibrous composites (Figure 2.10)

(B) Laminate composites (Figure 2.11)

(C) Particulate composites (Figure 2.12) (Jones, 1975)

2.4.2.1 Fibrous Composites
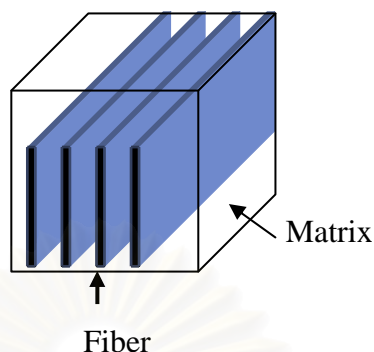
Figure 2.9 Fibrous composite structure.

        Fibrous composites consist of fibers of high strength and modulus embedded in or bonded to a matrix with distinct interfaces between them. Long fibers are inherently much stiffer and stronger than the same material in bulk. For example, plain plate glass fractures at stresses of only a few thousand psi; however, glass fibers have strengths of 400,000 to 700,000 psi in commercial fiber and about 1,000,000 psi in laboratory fiber (Jones, 1975). The geometry of a fiber is crucial and must be considered in applications. Moreover, the fiber has lower paradox than the bulk; since, the crystals are aligned in the fibers.

2.4.2.2 Laminate Composites
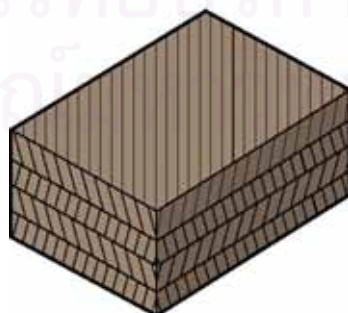
Figure 2.10 Laminate composite structure.

Laminate composites consist of layers of at least two different materials that are bonded together (Jones, 1975). Lamination is used to combine the best features of the constituent layers in order to achieve a more useful material. The properties that can be enhanced by lamination are strength, stiffness, low weight, corrosion resistance, wear resistance, beauty or attractiveness, thermal insulation, acoustical insulation, etc.

2.4.2.3 Particulate Composites
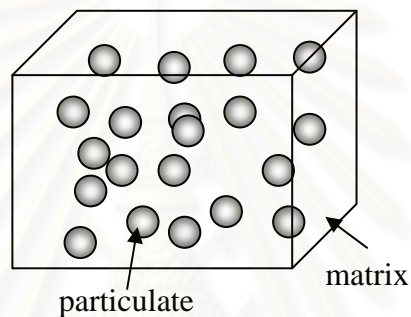
Figure 2.11 Particulate composite structure.

Particulates are the cheapest reinforcing materials. Particulate composites consist of particulates of one or more materials regularly suspended in the matrix. Hence, these composites are isotropic; that is, they have the same mechanical properties in all directions (Schwartz, 1996).

2.5 Adsorption

Adsorption is a process that occurs when adsorbate (gas or liquid solute) accumulates on the surface of adsorbent (solid or a liquid), forming film of molecules or atoms. In general, the adsorption on solid surface can proximately be classified into two categories. One is physisorption (or physical adsorption) and the other is chemisorption (or chemical adsorption).

2.5.1 Physisorption

Physisorption is mainly result of Van der Waals interactions between the molecules of adsorbing surface (the adsorbent) and adsorbate molecules. Van der Waals interactions are weak interactions. Moreover, the energy is released when adsorbate molecule is physisorbed, resulting in the formation of multilayers of adsorbate molecules. Physisorption usually occurs very rapidly at very low temperatures. Its characteristics are:

- low temperature: always under the critical temperature of the adsorbate
- type of interaction: Van der Waals forces
- low enthalpy: $\Delta H < 20$ kJ/mol
- adsorption in multilayers
- low activation energy
- not alteration of energy state of adsorbate
- reversible

2.5.2 Chemisorption

Chemisorption is a type of adsorption whereby a molecule adheres to a surface through the formation of a chemical bond; moreover, it is stronger than Van der Waals forces which cause physisorption. Its characteristics are:

- high temperatures

- type of interaction: covalent bond between adsorbate and surface

- high enthalpy: 50 kJ/mol $<\Delta H<$ 800 kJ/mol

- adsorption only in a monolayer

- high activation energy

- increase of electron density in the adsorbent-adsorbate interface

- reversible only at high temperature

2.5.3 Role of Intermolecular Force in Adsorption

2.5.3.1 Van der Waals Forces

These forces are weak interactions between the nuclei of the constituent atoms of one molecule with the electrons of another. The Van der Waals forces increase with increasing of the molecular size. They operate only when adsorbate and adsorbent molecules are in close proximity to each other; therefore, they can become dominant force attraction.

2.5.3.2 Hydrogen Bonds

The hydrogen atom is the smallest of entire the atoms, and in organic compounds. Hydrogen atom normally forms a single covalent bond only. Often, however, a neighboring atom may have a higher affinity for electrons than the hydrogen atom, causing a drift of the electrons shared by the hydrogen towards the larger atom. This leaves a slight positive charge on the hydrogen atom, which encourages bond formation between it and nearby atom such as nitrogen or oxygen. Such bonds are readily broken and re-formed and they are one of the factors involved when substances are dissolved by water.

2.5.3.3 Ionic Bonding or Salt Link

This attraction force is caused by electron transfer from one atom to another. The resulting ions have opposite charges, like the acidic and basic groups react together to form salt links.

2.5.3.4 Covalent Bonding

This bonding involves sharing of electrons, thus each atom has two electrons in its valence shell. Covalent bonding is stronger than salt link, hydrogen bond and Van der Waals force, respectively as shown in Table 2.3.

Table 2.3 Comparison of bond strength

Bond Type	Relative Strength
Van der Waals	1.0
Hydrogen bond	3.0
Ionic bond	7.0
Covalent bond	30.0

2.5.4 Type of Adsorption Isotherms

Adsorption isotherm is the relationship between the amount adsorbed by unit mass of solid and the equilibrium pressure (or relative pressure), at a known temperature. The experimental adsorption isotherm is usually presented in graphical form.

2.5.4.1 Physisorption of Gases

Experimental adsorption isotherms measured on variety of gas-solid systems, have several forms. Nevertheless, the majority of these isotherms resulted from physical adsorption may conveniently be grouped into six classes according to

the IUPAC classification as Figure 2.12. Type I to V were originally proposed by S. Brunauer, L.S. Deming, W.S. Deming and E. Teller as the BDDT classification, sometimes referred to as the Brunauer classification. Besides, type VI has been more recently observed (Rouqerol, Rouqerol, and Sing, 1999).
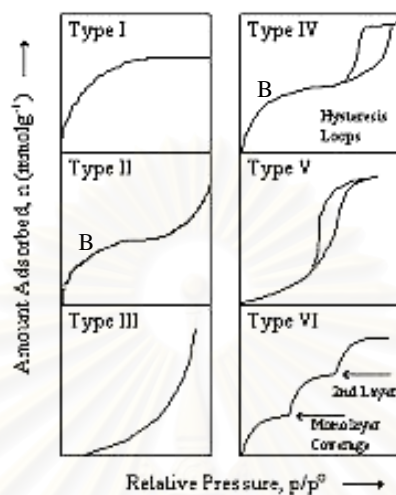
Figure 2.12 The six main types of gas physisorption isotherms, according to the
        IUPAC classification

Type I isotherm is concave to the relative pressure (P/P_o) axis. It rises sharply at low relative pressure and reaches a plateau at which amount adsorbed by the unit mass of solid approaches a limiting value as $P/P_o \rightarrow 1$.

The narrow range of relative pressure before reaching the plateau is an indication of a tiny pore size and the appearance of a nearly horizontal plateau indicates a very small external surface area. Hence, the limiting adsorption is dependent on the available micropore volume (Rouqerol *et al.*, 1999).

Type II isotherm is concave to the P/P_o axis, then almost linear and finally convex to the P/P_o axis. It indicates a formation of an adsorbed layer whose thickness increase progressively with increasing relative pressure until $P/P_o \rightarrow 1$. When the equilibrium pressure equals the saturation vapour pressure, the adsorbed layer becomes a bulk liquid or solid. If the knee of the isotherm is sharp, the uptake at Point B (the beginning of quasilinear section) is usually considered to represent completion of monomolecular layer (monolayer) and the beginning of formation of

multimolecular layer (multilayer). The ordinate of Point B gives an estimation of the amount of adsorbate required to cover the unit mass of solid surface with a complete monomolecular layer (monolayer capacity). Type II isotherm which is typical of non-porous or macroporous adsorbents occurs both monolayer and multilayer adsorption. If the adsorptive temperature is at or below the normal boiling point of the adsorbate, it is easy to establish the course of the adsorption-desorption isotherm over the entire range of P/P_o. The absence of adsorption hysteresis indicates the complete reversibility of this isotherm (Rouqerol *et al.*, 1999).

Type III isotherm is convex to the P/P_o axis over the complete range; therefore, it has no Point B. This feature, Figure 2.13, is indicative of weak adsorbent-adsorbate interactions (Rouqerol *et al.*, 1999).

Type IV isotherm, whose initial region is closely approached Type II isotherm, tends to level off at high relative pressures. It exhibits a hysteresis loop, the lower branch of which represents measurements obtained by progressive addition of the adsorbent, and the upper branch by progressive withdrawal. The hyteresis loop is generated by the capillary condensation of the adsorbate in the mesopores of the adsorbent. Moreover, the exact shape of the hyteresis loop depends on the shape of pore (Rouqerol *et al.*, 1999).

Type V isotherm is initially convex to the P/P_o axis and also levels off at high relative pressure. As in the case of the Type III isotherm, this is indicative of weak adsorbent-adsorbate interactions (Rouqerol *et al.*, 1999). However, the Type V isotherm exhibits a hysteresis loop which is associated with the mechanism of pore filling and emptying by the capillary condensation. Such isotherm is relatively rare.

Type VI isotherm, or stepped isotherm, is also relatively rare and is associated with layer-by-layer adsorption. The sharpness of the steps is dependent on the system and the temperature (Rouqerol *et al.*, 1999).

2.5.4.2 Chemisorption of Gases

Chemisorption isotherms generally exhibit a plateau at lower pressures than the micropore filling plateau. This limiting adsorption is due to the completion of a chemically bound monolayer. These isotherms may be referred to as Langmuir isotherms (Rouqerol *et al*., 1999); even if, the involved mechanism may not be strict in accordance with the Langmuir model. On the other hand, Langmuir isotherm should not be used to explain the physisorption by microporous solids. Obviously, the slow rate of chemisorption makes it difficult to obtain equilibrium data. Furthermore, the chemisorption reaction may be undetectable at low temperature or pressure.

2.5.4.3 Adsorption from Solution

A distinctive feature of adsorption from solution is that it always involves a completion of adsorption between the solvent and solute.

In this case, the apparent adsorption of a solute at the liquid-solid interface is usually evaluated by measuring the decrease of its concentration when the solute is brought to contact with the adsorbent. The adsorption isotherm is then plotted as the apparent adsorption of the solute against the equilibrium concentration.

2.6 Ascorbic Acid

Ascorbic acid, vitamin C, is an essential food and is required by human beings. This water-soluble vitamin is important in forming collagen, a protein that gives structure to bones, cartilage, muscle, and blood vessels. Its appearance is white to light-yellow crystals or powder with high solubility in water (pKa = 4.19). Ordinary ascorbic acid is also called L-ascorbic acid. There is another substance, D-ascorbic acid, that is closely related to L-ascorbic acid. In addition, these substances contain the same atoms, bond together similarly, but both forms are each other mirror images. The D and L-enantiomer indicate righthanded (dextro) and lefthanded (levo),

respectively. Only L-ascorbic acid has vitamin-C activity. The name of ascorbic acid without a prefix is used only in referring to L-ascorbic acid (Lewin, 1976).

2.6.1 Chemical and Structural Properties of Ascorbic Acid

L-ascorbic acid is an α-keto-lactone with a formula of $C_6H_6O_8$ and molecular weight of 176.13 g/mol. It contains a C=C bond between C-2 (or α) and C-3 (or β) carbons (Lewin, 1976). The chemical structure of ascorbic acid is revealed below.
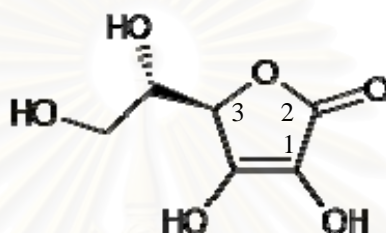
Figure 2.13 Chemical structure of ascorbic acid

Ascorbic acid has several types of oxidized derivative such as ascorbate anion ($C_6H_7O_6^-$) and dehydroascorbic acid ($C_6H_6O_6$). Besides, the chemical structures of both derivatives are shown in Figure 2.15 (a) and (b), respectively. The formation of ascorbate anion involves with ionization of C-2 OH group (Lewin, 1976). Moreover, ascorbic acid, a reducing agent, and ascorbate anion are readily converted into dehydroascorbic acid by oxidizing agents such as oxygen, ozone and halogen (Pauling, 1970). The reaction is reversible and is catalyzed by light and metal ion.
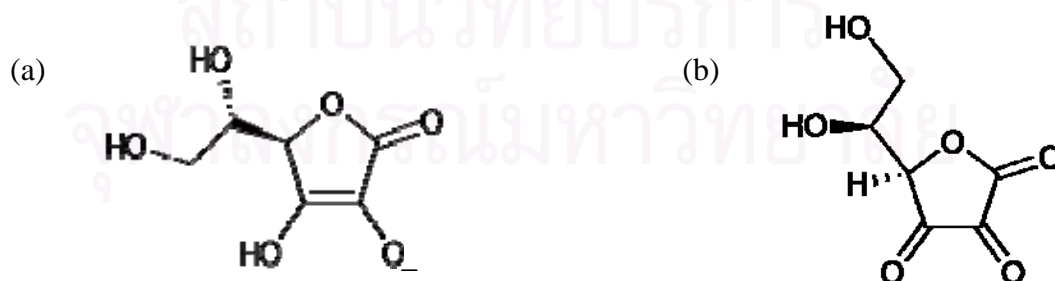
Figure 2.14 Chemical structures of (a) ascorbate anion and (b) dehydroascorbic acid

2.6.2 UV/Visible Absorbance

The UV/Visible absorbance band of ascorbic acid and its derivatives is due to the double bond between C-2 and C-3 (Lewin, 1976). As a result, the UV/Visible absorbance spectrum of the ascorbic acid differs clearly from that of ascorbate anion and dehydroascorbic acid because of difference of their ability of chromophore to adsorb light. Chromophore is a part of a colored organic compound responsible for light absorption.

2.6.2.1 Ascorbic Acid

The highest transmittance value (ε_{max}) reported for ascorbic acid in acidified solutions (HCl, pH 1.5) ranges between 10,500 and 12,220 at λ_{max} 244 nm (Lewin, 1976).

2.6.2.2 Ascorbate Anion

The optical absorbance spectrum of the ascorbate has been determined in several laboratories. The wavelength determined is 265.5 nm ± 0.3. Moreover, the value of ε_{max} ranges between 7,500 and 16,650 (Lewin, 1976).

2.6.2.3 Dehydroascorbic acid

Dehydroascorbic acid is transparent in the region of 230 nm to 280 nm, but has a weak absorption (ε_{max} = 720) at 300 nm (Lewin, 1976).

2.7 Literature Survey

In 2001, Chantippimarn *et al*. (Chantippimarn *et al*., 2001) studied the composite foam made from NR and sticky rice flour blends to establish a relationship

between the structure and physical properties. The blends of NR, sticky rice flour and other ingredients were prepared by mixing on a two-roll mill. Subsequently, foam structures of the blends were obtained by compression molding. It was found that density decreases with increasing flour loading, molding temperature and low cross-linking agent loading. Water absorption decreases with decreasing flour loading, molding temperature and cross-linking agent loading. Oil absorption decreases with decreasing molding temperature, cross-linking agent loading, and with flour loading less than 40%.

In 2002, Yodsoontorn *et al*. (Yodsoontorn *et al*., 2002) studied the influences of polar compounds, organic solvents (xylene, heptane, butyl acetate, octanol, propylene glycol) and temperature (30-60 ˚C) on the transport of organic solvents into natural rubber blended with polar compounds (chloroprene rubber, nitrile rubber, cassava starch) and the influence of polar compounds on mechanical properties. This work has shown that the transport of organic solvents into natural rubber is reduced if it is vulcanized. Adding a polar compound to NR improve markedly resistance to the transport of non-polar solvent. Polar solvent showed low sorption and diffusion into natural rubber.

In 2005, Arunyanad *et al*. (Arunyanad *et al*., 2005) studied adsorption of gaseous fuel on NR surface. The porous rubber was produced by using defrost technique from freezing latex. Aluminium silicate crystal formed by reaction between sodium silicate and aluminium sulfate, were acted as stabilizer. This study used the paraffin wax and carbon powder as the enhancement adsorption agent of hydrocarbon (LPG and methane) and hydrogen gas, respectively. The results presented that amount of adsorbed gas increased with increasing amount of adsorption agent and decreasing the temperature. For the desorption of gaseous fuel, it was found that time of gas desorption decrease when increasing amount of adsorption agent and decreasing of adsorption temperature.

In 2000, Imperor-Clerc *et al*. (Imperor-Clerc *et al*., 2000) studied the materials showing two-dimention hexagonal order (called SBA-15 in) that were produced by silica precursor (TEOS) as template and two types of Pluronic copolymer, $EO_xPO_yEO_x$, with nearly the same x/y (0.3) ratio but different y values (x=18, y=60

and x=20, y=70, respectively). These materials were hydrothermally treated to increase the condensation of silicate species around the Pluronic aggregates and calcined to liberate the template. The results presented that large number and narrow width of XRD powder diffraction lines demonstrate the good crystallographic quality of the materials. The structure of the silica walls is more complex and shows a "corona" region of lower density around the cylindrical organic aggregates. This corona becomes microporous upon calcination, and they suggested that it arises from the partial occlusion of the PEO chains in the silica matrix.

In 1997, Koyano *et al.* (Koyano *et al.*, 1997) showed that the stability of Si-MCM-48 to moisture and compression can be improved by trimethylsilylation; no hydrolytic cleavage of Si-O-Si bonds occurred on exposure to water vapor over a saturated aqueous solution of NH_4Cl at room temperature for 30 days, and the structure did not collapse upon applying external pressure of 1764 kg/cm^2. The high stability was attributed to the high hydrophobicity of Si-MCM-48(sil). Moreover, the stability was retained after removal of methyl groups by calcinations; although, the silylated-calcined material was low hydrophobic. The stabilization procedure is also applicable to Si-MCM-41 and Ti-containing mesoporous molecular sieves. The stability of Ti-MCM-41, which was very less resistant to moisture than pure-silica MCM-41, was drastically increased by similar treatment.

In 1999, Kwakye (Kwakye, 1999) studied the use of stabilizers in the UV assay of ascorbic acid. Sodium thiosulphate at a concentration of 0.04% w/v has been used to stabilize ascorbic acid in aqueous medium. The method has been used to assay ascorbic acid in commercial tablet preparations. It is very accurate, precise and reproducible. It compares favourably with titrimetric method. The method is simple and can be adopted for the routine assay of ascorbic acid in single component tablet formulations.

CHAPTER III

EXPERIMENTAL

3.1 Chemicals

3.1.1 Chemicals for Syntheses of Mesoporous Silicas

1. Fumed silica (SiO_2) (Aerosil 200, Degussa)
2. Sodium hydroxide (NaOH) (GR grade, MERCK)
3. Cetyltrimethylammonium bromide ($C_{16}H_{33}$)N(CH_3)$_3$Br) (Tokyo Chemical Industry)
4. Tetraethyl orthosilicate (Si(OC_2H_5)$_4$) (puriss, FLUKA)
5. Pluronic 123 block copolymer ($EO_{20}PO_{70}EO_{20}$)(commercial, BASF)
6. Hydrochloric acid (HCl) (AR grade, Fisher scientific)

3.1.2 Chemicals for Silylation

1. Silica gel (SiO_2) (for column chromatography, MERCK)
2. Trimethylcholosilane ((CH_3)$_3$SiCl) (puriss, FLUKA)
3. Hexamethyldisiloxane (((CH_3)$_3$Si)$_2$O) (puriss, FLUKA)
4. Acetone (CO(CH_3)$_2$) (AR grade, Fisher scientific)
5. Silica gel (SiO_2) (for column chromatography, MERCK)
6. Propyltrimethoxysilane ((CH_3O)$_3$Si(CH_2)$_2$-CH_3) (purum, FLUKA)
7. Isopropanol (C_3H_8O) (AR grade, Ajax finechem)

3.1.3 Chemicals for Preparation of NR Composite

1. Natural rubber ($(C_5H_8)_n$) (STR 5L, Thaihua Choomporn Rubber)
2. Toluene ($C_6H_5CH_3$) (AR grade, Fisher scientific)

3.1.4 Chemicals for Ascorbic Acid Adsorption

1. Ascorbic acid ($C_6H_8O_6$) (pure p.a., Poch)
2. Sodium thiosulphate pentahydrate ($Na_2S_2O_3 \cdot 5H_2O$)(AR grade,BDH)

3.2 Instruments and Equipments

3.2.1 Instruments and Equipments for Syntheses of Mesoporous Silica

1. Polyethylene beaker, 250 mL
2. Magnetic bar, 4 cm
3. Hotplate and magnetic stirrer
4. Dropper
5. Stirring rod
6. Teflon bottle, 250 mL
7. Oven
8. Aspirator pump
9. pH meter
10. Filter paper, No. 42
11. Muffle furnace
12. Beaker, 250 mL

3.2.2 Instruments and Equipments for Silylation

1. Three-necked round bottom flask, 250 mL
2. Magnetic bar, 2 cm

3. Heating mantle, 250 mL

4. Condenser

5. Thermometer

6. Glass stopper

7. Water pump

8. Rotary evaporator

9. Centrifuge

10. Oven

3.2.3 Instruments and Equipments for Preparation of NR Composite

1. Beaker, 50 mL

2. Magnetic bar, 2 cm

3. Hotplate and magnetic stirrer

4. Petri disc, inner diameter 9.5 cm

5. Oven

3.2.4 Instruments and Equipments for Ascorbic Acid Adsorption

1. Polypropylene volumetric flask, 25, 50, 100 mL

2. Polyethylene bottle, 125 mL

3. Magnetic bar, 2 cm

4. Aluminum foil

5. Hotplate and magnetic stirrer

3.2.5 Instruments and Equipments for Characterization of Silica
   Materials

3.2.5.1 X-ray Diffractometer

Structure of mesoporous silicas in this study (MCM-41 and SBA-15) was confirmed by a Bruker D8 Discover X-ray diffractometer equipped with Cu Kα radiation. The XRD patterns were collected at 2-theta from 0.5 to 5 degrees.

Figure 3.1 Bruker D8 Discover X-ray Diffractometer.

3.2.5.2. CHN Analyzer

Carbon and hydrogen contents of the silica gel both before and after the silylation were measured on a LECO CHN-2000 CHN Analyzer.

Figure 3.2 LECO CHN-2000 CHN Analyzer.

3.2.5.3. Surface Area and Porosity Analyzer

Micromeritics ASAP 2020 surface area and porosity analyzer was used for textural properties measurement of the silica materials both before and after the silylation.

Figure 3.3 Micromeritics ASAP 2020 Surface Area and Porosity Analyzer.

3.2.5.4. Fourier Transform Infrared Spectrometer

Fourier-transform infrared (FTIR) spectra were recorded on a Perkin Elmer FTIR spectrum RX-I Fourier Transform Infrared Spectrometer. Sample (2.5 mg) for FTIR analysis was prepared by mixing with KBr (50 mg). The obtained mixture (25 mg) was grounded and palletized by compression in the mould at 9 bar. For each spectrum, 16 scans at a resolution of 4 cm^{-1} in the range of wave number from 4000 cm^{-1} to 400 cm^{-1} were performed.
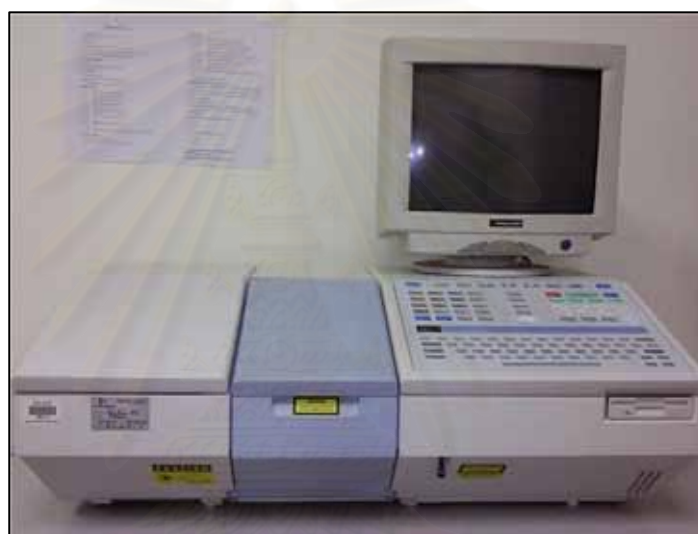
Figure 3.4 Perkin Elmer FTIR spectrum RX-I Fourier Transform Infrared Spectrometer.

3.2.6 Instruments and Equipments for Characterization of NR Composite

3.2.6.1 Surface Area and Porosity Analyzer

Textural properties of the NR Composites was measured on a Micromeritics ASAP 2020 Surface Area and Porosity Analyzer.

3.2.6.2 Scanning Electron Microscope

Characteristics of NR composites surface were observed by a JEOL JSM-5410 LN Scanning Electron Microscope (SEM). The sample was sputter-coated with gold before the observation. The SEM micrographs were taken by using a 15 kV electron beam with a magnification of 150 – 20,000. The SEM micrographs were used to determine morphology of silica materials and distribution of silica materials in NR composites.

Figure 3.5 JEOL JSM-5410 LN Scanning Electron Microscope.

3.2.6.3 Thermogravimetric/Differential Thermal Analyzer.

Thermogravimetric analysis (TGA) of NR composite was carried out by using a Perkin Elmer Pyris Diamond Thermogravimetric/Differential thermal Analyzer to determine the silica material contents of NR composites. Typically, 10 mg of a sample was placed in a platinum pan and heated from room temperature to 1,000 °C at a heating rate of 10 °C/min with air flow rate of 50 mL/min.

Figure 3.6 Perkin Elmer Pyris Diamond Thermogravimetric/Differential Thermal Analyzer.

3.2.7 Instruments and Equipments for Adsorption Characterization

3.2.7.1 UV/Vis Spectrophotometer

Concentration of ascorbic acid was calculated from absorbance of desorbed ascorbic acid solution measured in a JUSCO V-530 UV/Vis Spectrophotometer. Moreover, it was calculated from Beer's law:

$A = \log \underline{I}_0$; A = absorbance

        I I_0 = incident light

             I = transmitted light

$A = \varepsilon bc$; ε = absorptivity

             b = cuvette width

             c = sample concentration
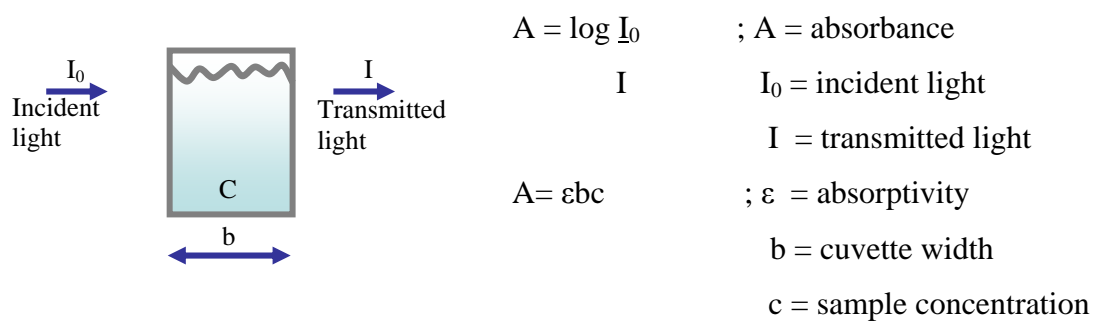
Figure 3.7 Transport of light through cuvette.

The optical absorption spectrum of ascorbic acid was revealed highest wavelength value (λ_m) at 264 nm determined using sodium thiosulphate blank solution.
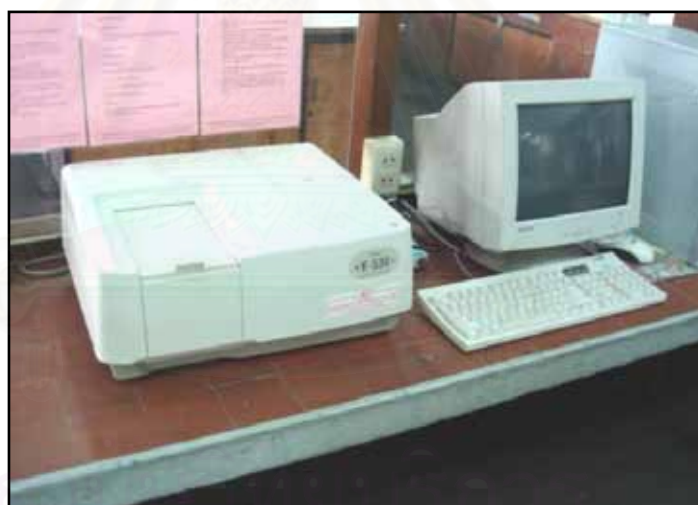
Figure 3.8 JUSCO V-530 UV/Vis Spectrophotometer.

3.3 Syntheses of Mesoporous Silicas

3.3.1 MCM-41 (Avelino, Qiubin, and Maria, 1997)
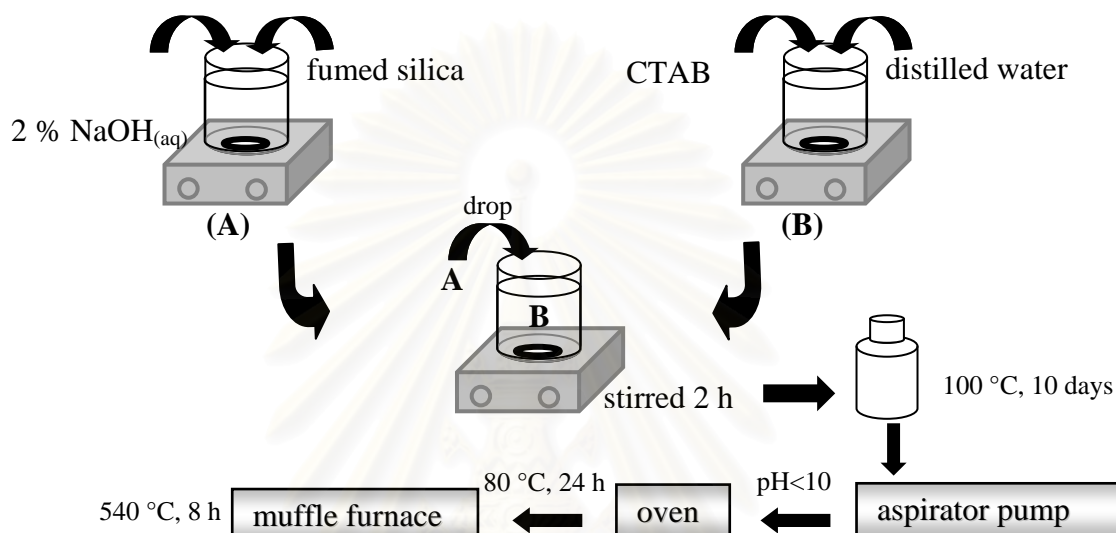
Scheme 3.1 MCM-41 synthesis procedure.

In a typical synthesis, an aqueous mixture of 7 g of fumed silica and 65.24 g of 2 wt% NaOH aqueous solution, was added to an aqueous solution containing 51.58 g of 9.86 wt% cetyltrimethylammonium bromide (CTAB) solution under vigorous stirring at ambient temperature for 2 h. Subsequently, the resultant gel was poured into a Teflon bottle and heated under static conditions at 100 °C for 10 days. After the hydrothermal treatment, the solid was filtered, washed with deionized water, and dried at 80 °C overnight. Finally, it was calcined in a muffle furnace at 540 °C for 8 h in order to remove the template.

3.3.2 SBA-15 (Imperor-Clerc, Davidson, and Davidson, 2000)
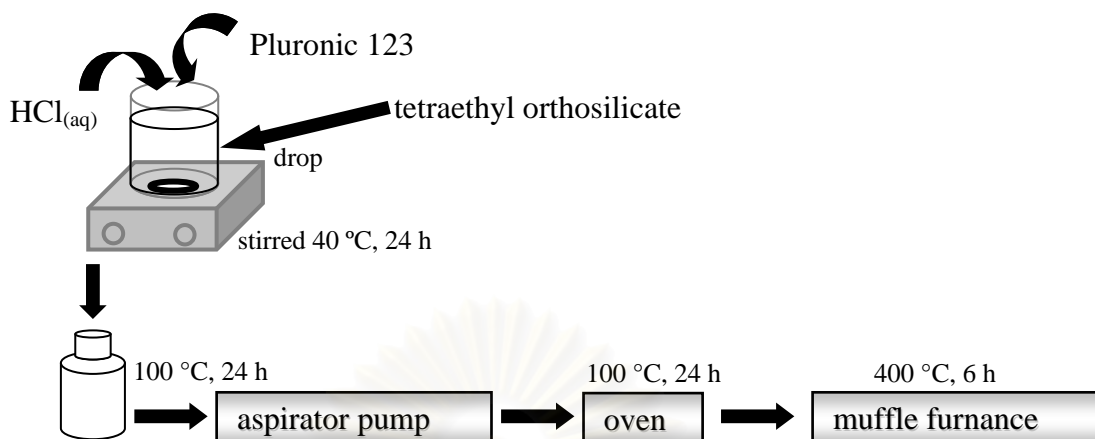
Scheme 3.2 SBA-15 synthesis procedure.

SBA-15 was synthesized by using Pluronic 123 (poly(ethylene oxide)-poly(propylene oxide)- poly(ethylene oxide) $EO_{20}PO_{70}EO_{20}$, P123) triblock copolymer as the template and tetraethyl orthosilicate (TEOS) as the silicate source. In a typical synthesis, 4 g of Pluronic 123 was dissolved in a mixture of 116.28 mL of deionized water and 8.76 g of HCl under vigorous stirring at 40 °C followed by the addition of 8.52 g of TEOS. The resultant mixture was maintained at the same temperature for 24 h. Subsequently, it was submitted to a hydrothermal treatment at 100 °C for 1 day. After recovery of the solid product by filtration, it was dried at 100 °C for 1 day. Finally, the dried solid was calcined in a muffle furnace at 400 °C for 6 h in order to remove the template.

3.4 Preparation of Silica Gel
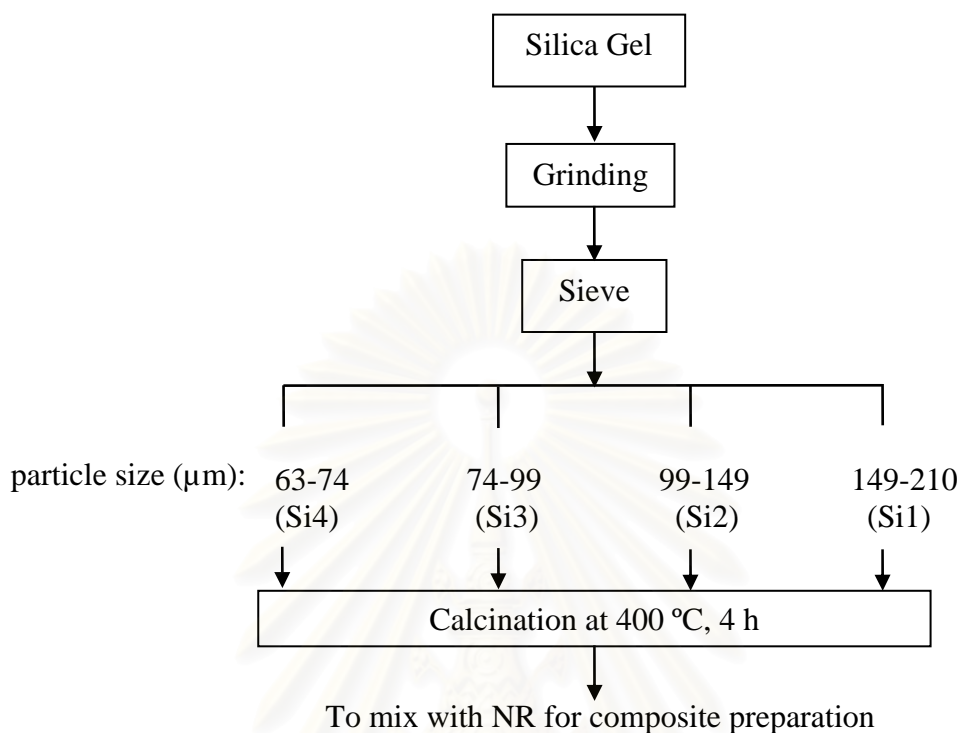
Scheme 3.3 Preparation of silica gel procedure.

This study also concern about influence of silica gel size on textural and adsorptive properties of NR composite. First stage of the classification, all size of silica gel were grinded by a mortar; then, these were sieved by the sieve (size 100, 150 and 200 mesh, respectively). Consequently, there are four silica gel sizes were 149-210 (Si1), 99-149 (Si2), 74-99 (Si3) and 63-74 (Si4). Finally, all sizes of silica gel were calcined to eradicate humidity and impurity at 400 °C for 4 h. These products were conserved in dessicator cabinet to mix with NR for composite preparation

3.5 Silylation

3.5.1 Trimethylsilylation (TS) (Koyano *et al.*, 1997)
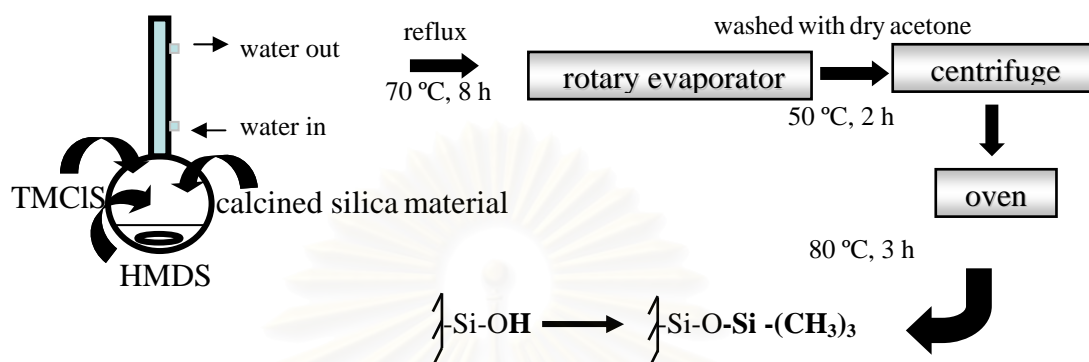
Scheme 3.4 Trimethylsilylation.

In a typical surface modification, 1 g of calcined silica material, 10 g of $(CH_3)_3SiCl$, TMClS, and 15 g of $((CH_3)_3Si)_2O$, HMDS were refluxed at 70 °C for 7 h. The reaction mixture was then loaded into a rotary evaporator to remove the solvent. The dried powder was washed with 10 mL of dry acetone. Then the solid was recovered by centrifuge and dried at 80 °C for 3 h. Then, the samples before and after the trimethylsilylation are designated as Si and Si-S1, respectively.

3.5.2 Propylsilylation (PS) (Yokoi, Tatsumi and Yoshitake, 2004)
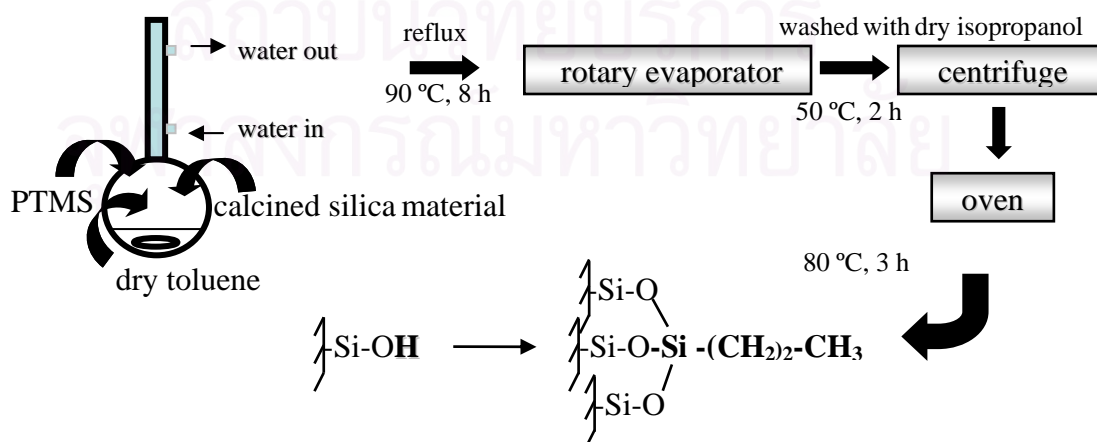
Scheme 3.5 Propylsilylation.

Typically, 3 g of a calcined sample, 2.46 g of $(CH_3O)_3Si(CH_2)_2$-CH_3 (PTMS), and 30 g of dry toluene $(C_6H_5CH_3)$ were refluxed at 70 °C for 7 h. The reaction mixture was then loaded into a rotary evaporator to remove the solvent. The dried powder was washed with 10 mL of dry isopropanol. Then the solid was recovered by centrifuge and dried at 80 °C for 3 h. Hereafter, the samples before and after the propylsilylation are designated as Si and Si-S2, respectively.

3.6 Preparation of NR Composite

This study prepared NR composite via two methods. The first method, each size and type of the silica materials before and after surface modification by silylation were mixed with NR by a two–roll mill. Total mixing time was 20 min at ambient temperature. The thickness of NR composite was controlled at 1.5 mm. The other method is slurry technique. The silica material was added to 15 g of 2.8 wt% NR solution dissolved in toluene under vigorous stirring at ambient temperature for 1 h. Subsequently, the resultant mixture was poured into a Petri disc to form a thin film; then, the film was dried in three stages at 80, 95 and 111 °C for 20 min in each stage. The thickness of the final product was between 0.35- 0.45 mm. Consequently, silica materials content was ranged from 100 to 300 phr. Table 3.1 shows blending formulation of preparation of NR composite via both methods. Designation of composite name is NR/X(Y) where X represent silica material type and Y represent silica material content.

Table 3.1 Blending Formulation of Silica Materials and NR

Sample (phr)	NR/X(50)	NR/X(80)	NR/X(100)	NR/X(200)	NR/X(300)
natural rubber	100	100	100	100	100
silica materials	50	80	100	200	300

X: silica material type

phr: part per hundred part of rubber

3.7 Ascorbic Acid Adsorption

Capability of ascorbic acid adsorption of NR composite was considered from amount of ascorbic acid adsorbed and desorbed by NR composite. Before being applied to the adsorption, a NR composite was cut into a quadrate (1.5 x 1.5 cm^2) and weighted. The adsorption of 0.2 % w/v ascorbic acid was conducted in a 125 mL polyethylene bottle equipped with a magnetic stirrer. The cut NR composite was dipped in ascorbic acid aqueous solution at ambient temperature for 15 min. During the adsorption, the polyethylene bottle was wrapped with aluminum foil to prevent photo-oxidation of ascorbic acid. Subsequently, the wet composite was dipped in 0.05% (w/v) $Na_2S_2O_3$ aqueous solution as the ascorbic acid stabilizer at ambient temperature for 15 min to desorb ascorbic acid from the film. The amount of desorbed ascorbic acid was measured by using a UV/Vis spectrophotometer.

CHAPTER IV

RESULTS AND DISCUSSION

4.1 Characterization of Silica Materials

Pure silica materials used in this work were silica gel and mesoporous silicas such as MCM-41 and SBA-15. It was important to characterize textural properties of these silica materials; because, their adsorption property concentrated on this work might involve with their textural properties. Moreover, to confirm structure of prepared mesoporous silica, X-ray diffraction analysis was used to characterize.

4.1.1 Characterization of Pure Silica Materials

4.1.1.1 Textural Properties of Pure Silica Materials

The textural properties of silica materials were determined by N_2 adsorption–desorption technique by using a Surface Area and Porosity Analyzer. As shown in Table 4.1, in comparison with NR, BET surface area and average pore volume of all types of pure silica materials were much higher. Both BET surface area and average pore volume decreased with the particle size of silica gel; since, grinding particle Si1 to prepare Si4 with smaller size broke the parent porous particles resulting in loss of porosity as well as specific surface area. An increase in the average pore size should be derived from an interparticle void. The N_2 adsorption–desorption isotherms of Si1 and Si4 are shown in Figure 4.1. Both materials exhibited type IV adsorption isotherms with a hysteresis loop in the mesopore region.

The isotherms of both MCM-41 and SBA-15 are shown in Figures 4.2 and 4.3, respectively. Both materials present type IV adsorption isotherm with a hysteresis loop in the mesopore region. The isotherm of MCM-41 was also studied by

Araujo and Jaroniec (2000). They indicated that MCM-41 had higher adsorption quantity and a hysteresis loop occurred at higher P/P_0 than one of material prepared in this study. SBA-15 was also studied by Linhua *et al.* (2000). This literature also revealed higher quantity adsorbed and higher P/P_0 of occurrent a hysteresis loop. These results might be affected from different preparation methods. Both calcined and uncalcined materials, MCM-41 had higher quantity adsorbed than SBA-15, but the hysteresis loop of MCM-41 occurred at lower P/P_0 resulting in higher BET surface area but lower average pore diameter of MCM-41 (Yang, 2003) as shown in Table 4.1. The isotherms of both calcined and uncalcined materials are also compared in these figures. The uncalcined materials had lower adsorption quantity; since, template molecule remained in structure resulting in lower porosity (Berube and Kaliaguine, 2008) as also presented in Table 4.1.

Table 4.1 Textural Properties of Pure Silica Materials

Sample	Particle size[a] (μm)	S_{BET}[b] ($m^2\ g^{-1}$)	V_P[c] ($cm^3\ g^{-1}$)	D_p[d] (Å)
NR[e]	n.d.[h]	7	0.003	41.2
Si1	149-210	468	0.677	45.9
Si4	63-74	392	0.654	57.1
MCM-41-uncal[f]	0.5-0.7	398	0.363	20.9
MCM-41-cal[g]	0.3-0.5	838	0.789	22.9
SBA-15-uncal[f]	1.5-2.0	369	0.335	21.1
SBA-15-cal[g]	1.0-1.5	775	0.780	55.1

[a] Determined by SEM.

[b] BET surface area.

[c] Average pore volume.

[d] Average pore size.

[e] Natural rubber.

[f] Uncalcined silica material.

[g] Calcined silica material.

[h] Represented not determine.
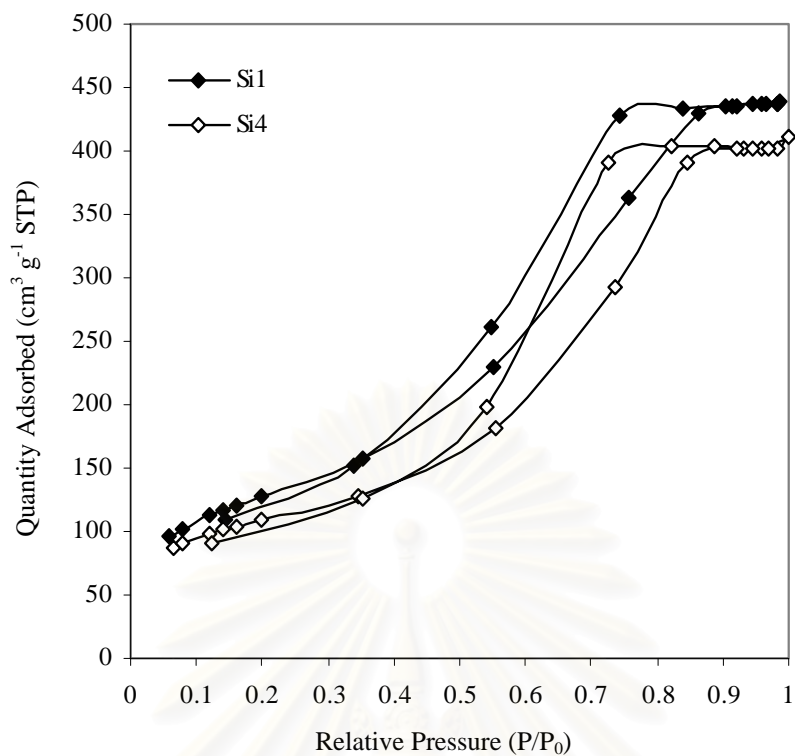
Figure 4.1 N_2 adsorption-desorption isotherms of Si1 and Si4.
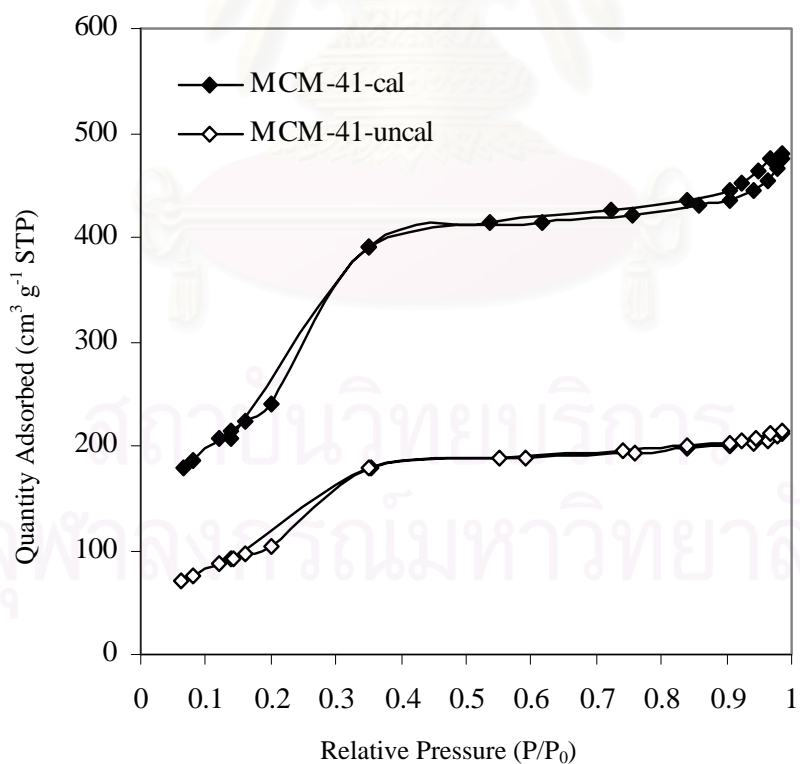
Figure 4.2 N_2 adsorption-desorption isotherms of MCM-41-cal and MCM-41-uncal.
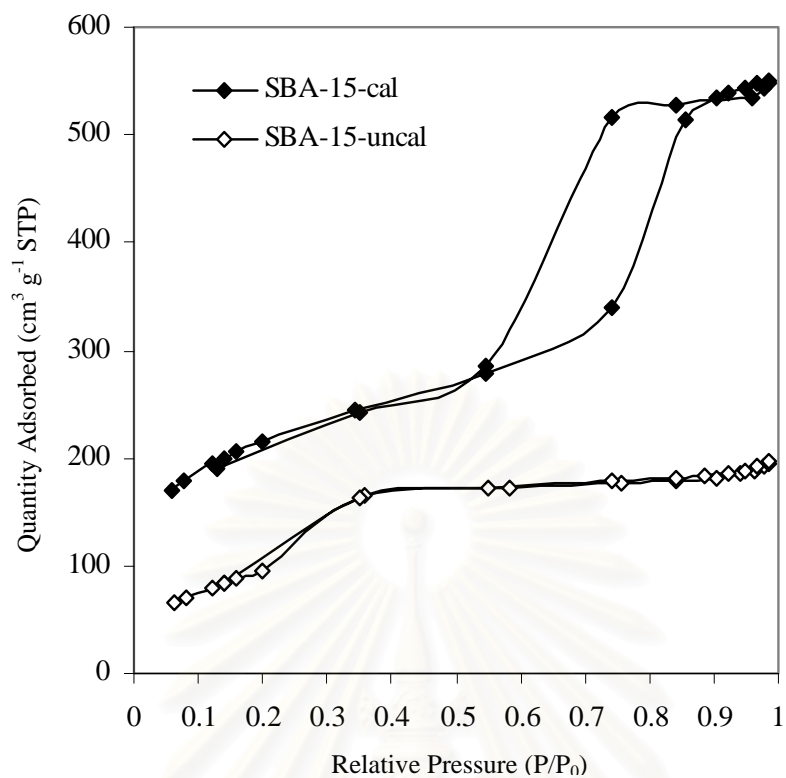
Figure 4.3 N_2 adsorption-desorption isotherms of SBA-15-cal and SBA-15-uncal.

4.1.1.2 Structure and Crystallinity of Synthesized Mesoporous Silica

Figure 4.4 shows XRD patterns of both calcined and uncalcined MCM-41. The XRD pattern of uncalcined material presents four peaks at $2\theta = 2.0°$, 3.7°, 4.2° and 5.5° which can be indexed to (100), (110), (200) and (210) reflections assuming a hexagonal unit cell. In addition, the XRD pattern of calcined MCM-41 shows three peaks at $2\theta = 2.4°$, 4.1° and 4.7. The most prominent peak at $2\theta = 2.4°$ could be also attributed to (100) reflection. The other reflections can be indexed as (110) and (200) reflections also indexed to its typical hexagonal unit cell. After calcination of MCM-41, the increase of X-ray reflections intensity indicated increasingly density of structure and slightly shift to higher angle corresponded to a decrease lattice constant. These results indicated that synthesized both calcined and uncalined materials of MCM-41 had a hexagonal unit cell (Elizabeth *et al*., 2006).
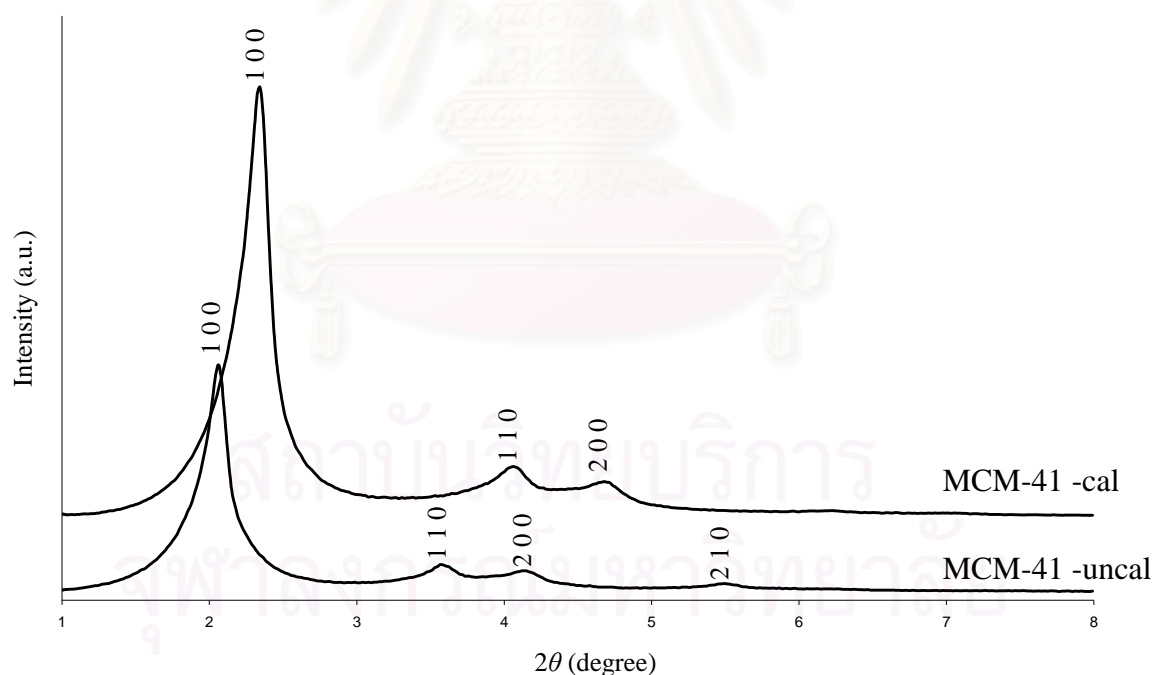
Figure 4.4 XRD patterns of uncalcined MCM-41 and MCM-41 calcined at 540 °Cθ

XRD patterns of both calcined and uncalcined SBA-15 were shown in Figure 4.5. The XRD pattern of uncalcined SBA-15 presents four peaks at $2\theta = 0.8°$, 1.4°, 1.7° and 2.55°. Though, five peaks of XRD pattern of calcined material less shift to higher angles at $2\theta = 0.85°$, 1.43°, 1.75°, 2.25° and 2.65°. which might be associated with the (100), (110), (200), (210) and (211) reflections. Oscar *et al.* (2007) presented XRD patterns of both SBA-1 and SBA-15. It was found that diffractogram of SBA-1 showed three peaks indexed to (200), (210) and (211) reflections and that of SBA-15 showed identical reflections of MCM-41. Therefore, it implied that prepared material might be a mixture of both SBA-1 and SBA-15.
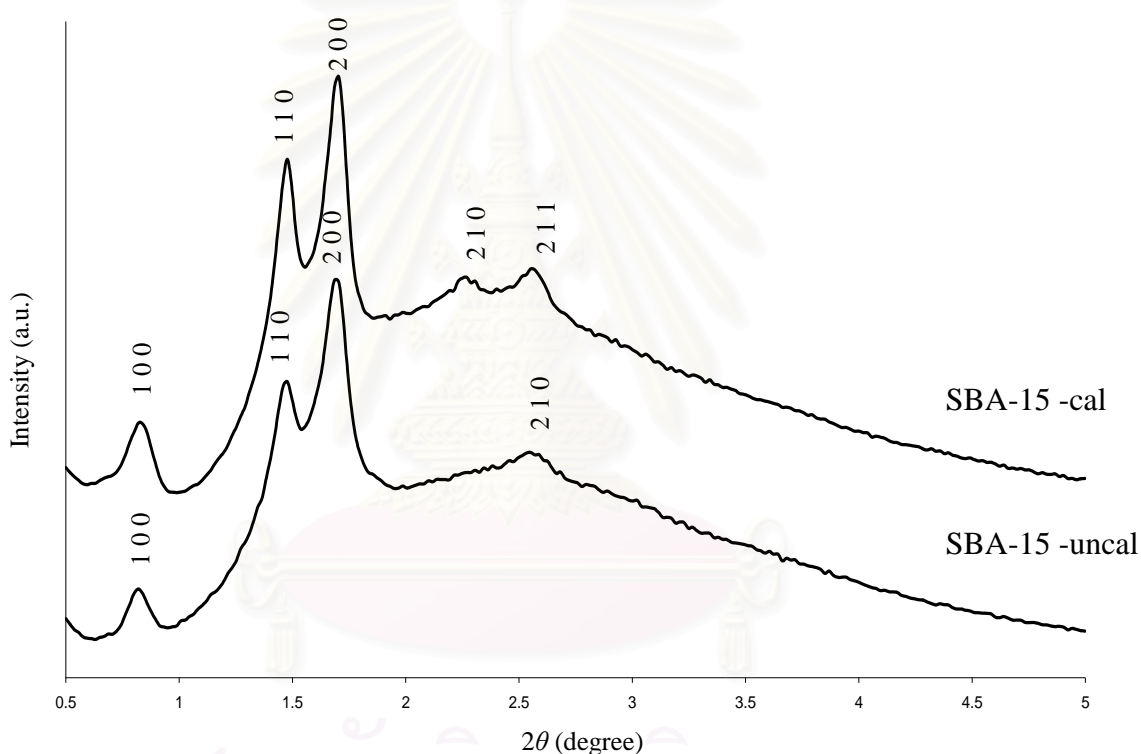
Figure 4.5 XRD patterns of uncalcined SBA-15 and SBA-15 calcined at 400 °C.

4.1.2 Characterization of Functionalized Silica Materials

In NR composite, to prevent the phase separation between the hydrophilic NR and hydrophobic silica material, it was concentrated on surface functionalization of silica materials to improve compatibility between two parts.

4.1.2.1 Textural Properties of Functionalized Silica Materials

Textural properties of functionalized silica materials by trimethylsilylation are summarized in Table 4.2, in comparison with parent silica material, BET surface area, average pore volume and average pore size of functionalized particles were lower. These results may be ascribed that organosilane covered some porosity in silica material structure. It indicate that the surface functionalization decrease porosity of finish materials.

Table 4.2 Textural Properties of Silica Materials and Functionalized Silica Materials

Si4	Textural properties		
	$S_{BET}{}^a$ (m^2 g^{-1})	$V_p{}^b$ (cm^3 g^{-1})	$D_p{}^c$ (Å)
Before TS^d	392	0.654	57.1
After TS^e	315	0.477	40.9

^{a} BET surface area.

^{b} Average pore volume.

^{c} Average pore size.

^{d} Before trimethylsilylation.

^{e} After trimethylsilylation.

4.1.2.2 Elemental Composition of Functionalized Silica Materials

To confirm that both types of functionalization were occurred on surface of silica gels, carbon and hydrogen composition of functionalized silica gel by trimethylsilylation were determined by CHN analyzer. As revealed in Table 4.3 it

indicated that C:H atomic ratio of functionalized silica gels with various size (Si1-TS to Si4-TS) were more than one of Si0 as parent silica gel. Also, C:H atomic ratio of all sizes of functionalized silica gel was about 0.33 which was approximately that of trimethylcholosilane (C:H atomic ratio ~ 0.333) as organosilane. Hence, this result implied that trimethylsilylation occurred on silica gels surface resulting in. an increase of hydrophilicity on silica surface (Koyano et al., 1997).

Table 4.4 shows carbon and hydrogen compositions of functionalized silica gels by propylsilylation. C:H atomic ratio of functionalized silica gels with various sizes was similar to 0.36 which was less than one of propyltrimethoxysilane (C:H atomic ratio = 0.43) as organosilane. However, this atomic ratio was close to atomic ratio of isopropanol solvent for sample washing after functionalization. It was ascribed that this solvent still remained on surface of functionalized particle. Then, it implied that both types of surface functionalizations of silica gel were able to increase hydrophilicity of silica surface.

Table 4.3 Elemental Composition in Structure of Functionalized Silica Gel by
Trimethylsilylation

Sample	Elemental Composition		
	Carbon (wt.%)	Hydrogen (wt.%)	C:H Atomic Ratio
Si0[a]	0.043	1.400	0.003
Si1-TS[b]	6.506	1.633	0.332
Si2-TS[b]	5.730	1.572	0.304
Si3-TS[b]	5.424	1.571	0.288
Si4-TS[b]	7.500	1.915	0.326

[a] Unfunctionalized silica gel.

[b] Silica gel functionalized by trimethylsilylation.

Table 4.4 Elemental Composition in Structure of Functionalized Silica Gel by
Propylsilylation

	Elemental Composition		
Sample	Carbon	Hydrogen	C:H
	(wt.%)	(wt.%)	Atomic Ratio
Si0[a]	0.043	1.400	0.003
Si1-PS[b]	8.638	4.584	0.370
Si2-PS[b]	6.505	1.515	0.358
Si3-PS[b]	5.801	3.214	0.350
Si4-PS[b]	6.110	1.438	0.354

[a] Unfunctionalized silica gel.

[b] Silica gel functionalized by propylsilylation.

4.1.2.3 Structure Characterization of Functionalized Silica Materials

The structures of silica gel and silica gels functionalized by trimetylsilylation and propylsilylation were characterized by FTIR spectroscopy. The characteristic FTIR spectra of parent silica gel as shown in Figure 4.6, the bands at 3505, 3454, and 3414 cm^{-1} may be ascribed to isolated silanol groups (Si-OH), geminal groups (Si-(OH)$_2$) and hydrogen-bonded Si-OH groups, respectively (Kierys, Pasieczna, Ryczkowski, and Goworek, 2006). Moreover, it also showed that the absorption band corresponding to the Si-O stretching of Si-O-Si and Si-OH and symmetric Si-O-Si stretching were located at 1053, 969 and 473 cm^{-1}, respectively.

For characteristic FTIR spectra of silica gels functionalized by trimetylsilylation (Si1-TS to Si4-TS) as shown in Figure 4.7 (a) to (d), the absorbance bands around 3300 to 3500 cm^{-1} (O-H stretching) remained after the functionalization corresponding to the incomplete reaction between silica gel and trimethylchlolosilane. Moreover, these samples were observed that the new absorption bands appeared at 2930, 1360 and 811 cm^{-1} corresponding to the C-H stretching, C-H blending of CH$_3$ stretching and Si-C stretching, respectively (Li, Shi, Dong, Qian, and Wei, 2009).

This indicated the partiality of functionalyzation of trimethyl group onto silica structure. For characteristic FTIR spectra of silica gels functionalized by propylsilylation (Si1-PS to Si4-PS) as shown in Figure 4.8 (a) to (d), the absorbance bands around 3300 to 3500 cm^{-1} (O-H stretching) also remained after the functionalization corresponding to the incomplete reaction between silica gel and propyltrimethoxysilane. Furthermore, these samples were also observed that the new absorption bands were appeared at 2860 and 1442 cm^{-1} corresponding to the C-H stretching and blending of CH$_2$. This indicated the partiality of this functionalyzation.
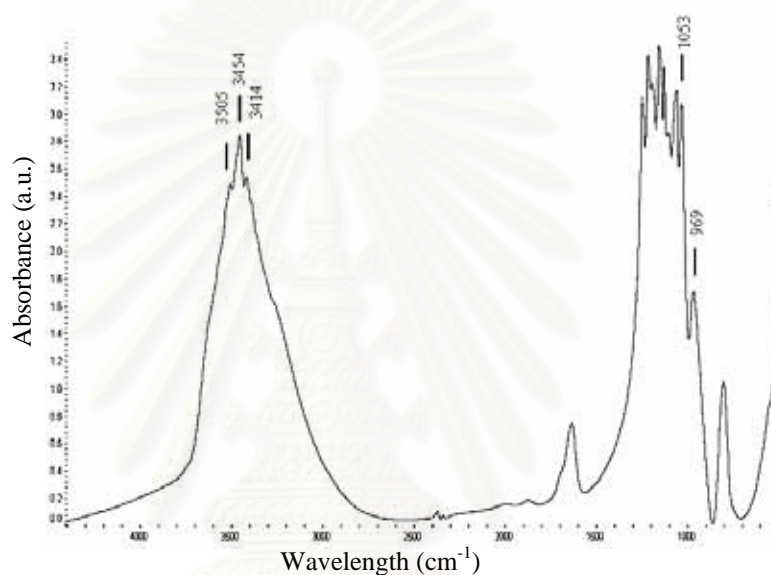
Figure 4.6 FTIR spectra of parent silica.
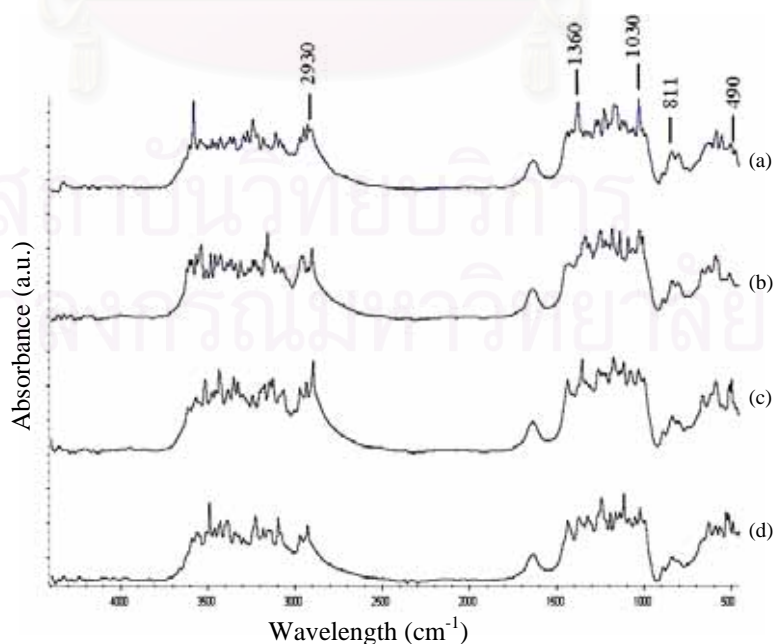
Figure 4.7 FTIR spectra of (a) Si1-TS, (b) Si2-TS, (c) Si3-TS and (d) Si4-TS.
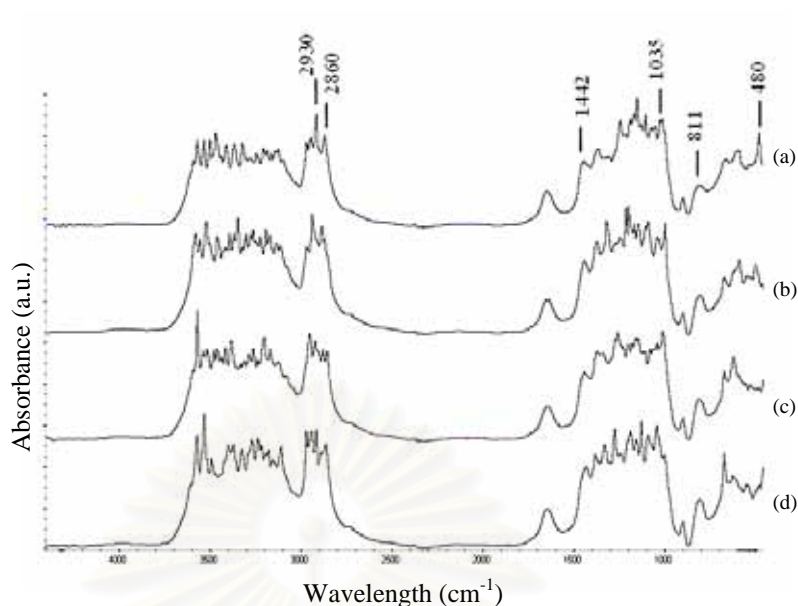
Figure 4.8 FTIR spectra of (a) Si1-PS, (b) Si2-PS, (c) Si3-PS and (d) Si4-PS.

4.2 Characterization of NR Composites

4.2.1 Appearance of NR Composites

4.2.1.1 Appearance of NR Composite Prepared by Two-roll Mill Mixing

After preparation of NR/Si4(5) composite by two-roll mill mixing, Figure 4.9 shows resulting composite that was sheet with 2.5 mm of thickness. Furthermore, it revealed aggregate of silica material dispersed ununiformly. This indicated that this technique was not appropriate to prepare NR composite with well particle dispersion.
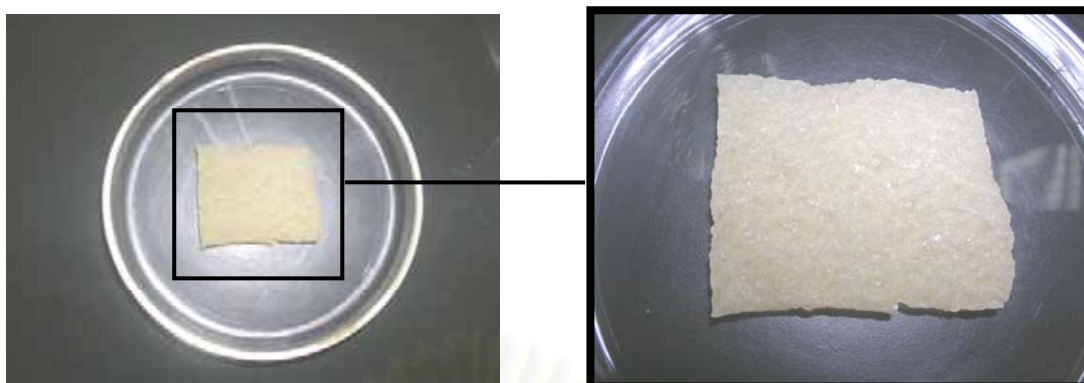
Figure 4.9 NR/Si4 composite (NR/Si4(5)) with silica content of 5 phr.

4.2.1.2 Appearance of NR Composite Prepared by Slurry
Technique

After preparation of NR/Si4 composite (NR/Si4(50)) with silica content of 50 phr by slurry technique, in Figure 4.10, it can be clearly seen that resulting composite was thin film with 0.3 mm of thickness. Furthermore, it revealed regular dispersion of silica material more than NR composite prepared by two-roll mill mixing. This research then used slurry technique to prepare NR composite.

Figure 4.10 NR/Si4 composite (NR/Si4(50)) with silica content of 50 phr.

4.2.2 Morphology of NR Composites

4.2.2.1 Morphology of NR Composite Prepared by Two-roll Mill Mixing

The SEM micrograph of NR/Si1(5) prepared by two-roll mill mixing were revealed in Figure 4.11 at 150 magnification. The white and gray tone color presented silica reinforcing material and the black tone color show NR matrix, respectively. In Figure 4.11, it can clearly be seen that some part of surface area of silica gel was covered by NR shown in mark of broken line and some silica particles were aggregated in mark of full line. This aggregate also built interparticle pore. Furthermore, it can be seen that size of silica particle in NR composite was smaller than 10 µm and smaller than its size before mixing (149-210 µm). This result suggested that preparation of NR composite by two-roll mill mixing resulted in silica material particle to break along mixing process and porous surface of silica material was covered by NR. Thus, two-roll mill mixing was not proper for increasing NR porosity.
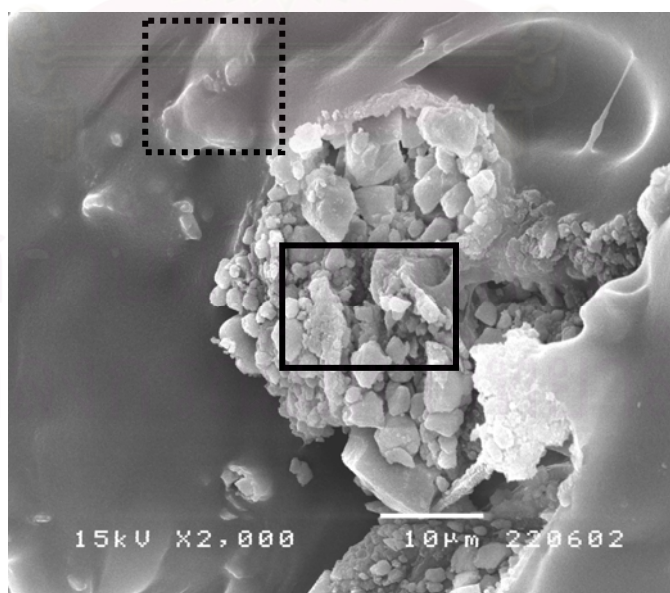
Figure 4.11 SEM micrograph of NR composite prepared by two-roll mill mixing: NR/Si1(5) (at 150 magnification).

4.2.2.2 Distribution of Silica Materials in NR Composites Prepared by Slurry Technique

The SEM micrographs of NR/Si1 composite (NR/Si1(200)) and NR/Si4 composite (NR/Si4(200)) with silica content of 200 phr that were prepared by slurry technique were revealed in Figure 4.12 (a) and (b), respectively at 150 magnification. Both Figures indicated that some part of surface area of silica was covered by NR in marks of broken line. Moreover, some silica particle beetled from NR surface was aggregated and built inter particle pore in marks of full line.

To observe influence of silica material sizes on distribution of silica reinforcing materials in NR composites, Figure 4.12 (a) and (b) were compared. It can be clearly seen that silica gel with smaller size (Si4) can increasingly issue from NR surface. This result was implied that, in equal weight, amount of smaller particle size (Si4) was more than that of larger size (Si1) as shown in Figure 4.12 (a). Thus, Si4 particles might be more overlapped and then these particles can increasingly issue from NR surface.
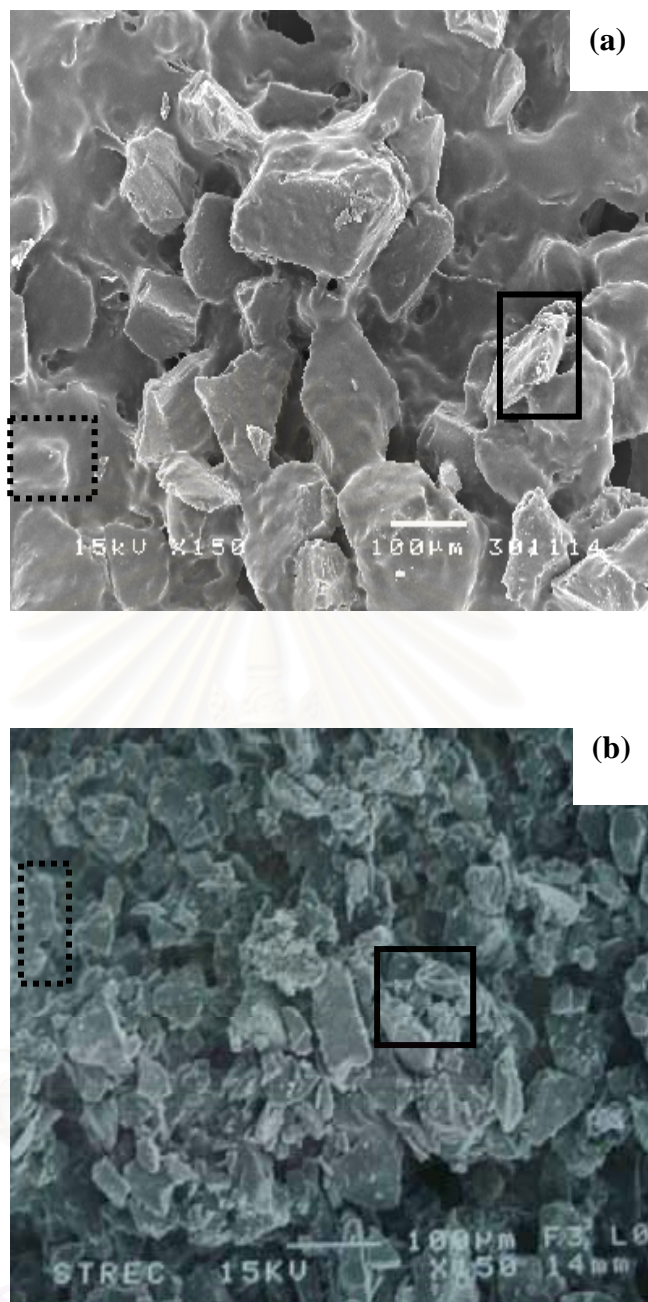
Figure 4.12 SEM micrographs of NR composite prepared by slurry technique: (a) NR/Si1(200) and (b) NR/Si4(200)

To investigate influence of content of silica material on distribution of silica reinforcing material in NR composite, the SEM micrographs of NR composite filled with Si4 of 100, 200 and 300 phr were revealed in Figure 4.13 (a), (b) and (c), respectively at 150 magnification. It can be clearly seen that, in Figure 4.13 (c), 300 phr of silica gel can increasingly thread NR surface when compared to 150 phr in Figure 4.13 (a) and 200 phr in Figure 4.13 (b) of silica gel in NR composite. It shows that content of silica gel increases with increasing the obtrusion of silica particle from NR surface.
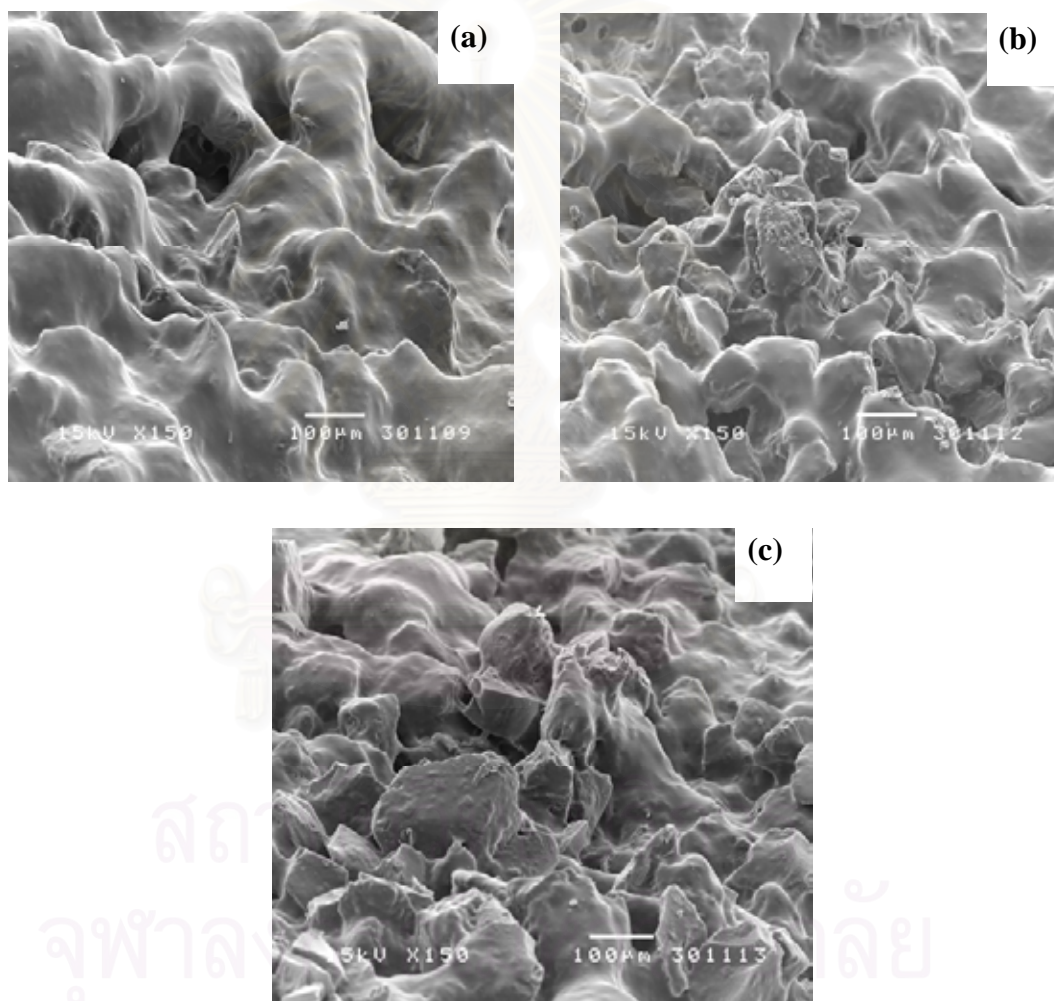
Figure 4.13 SEM micrographs of NR composite prepared by slurry technique:
(a) NR/Si4(100), (b) NR/Si4(200) and (c) NR/Si4(300) (at 150 magnification).

Morphology of NR composites filled with mesoporous silica such as SBA-15-uncal, SBA-15-cal, MCM-41-uncal and MCM-41-cal of 100 phr were revealed in Figure 4.14 (a), (b), (c) and (d), respectively at 150 magnification and. It can be clearly seen that packing of both types of uncalcined mesoporous silicas in Figure 4.14 (a) and (c) were looser than ones that consisted of calcined mesoporous silicas in Figure 4.14 (b) and (d). This result may be also due to template molecule remained in structure of uncalcined mesoporous silicas that obstructed flow of NR solution in mixing process. Then, it caused loose particles packing in NR composite that might build higher size of interparticle pore.
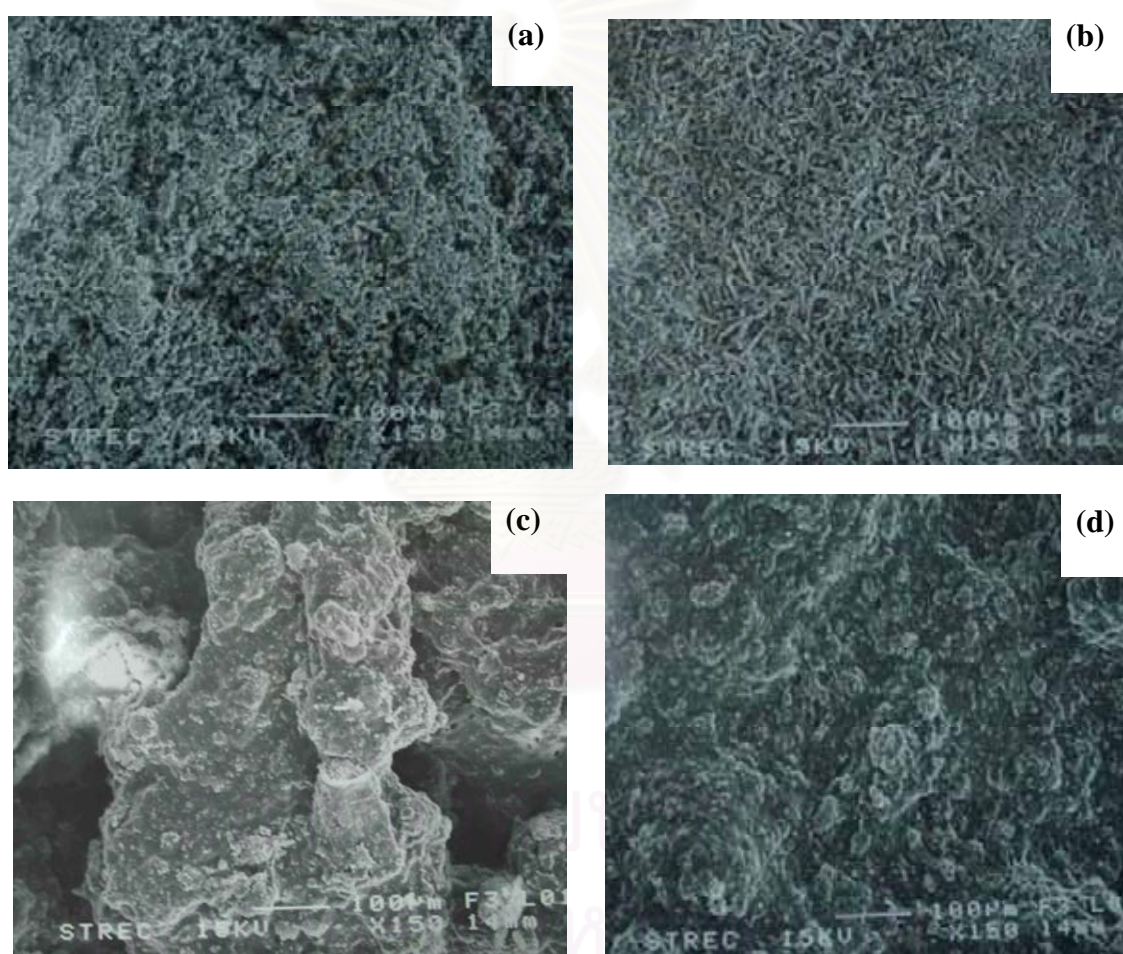
Figure 4.14 SEM micrographs of NR composite: (a) NR/SBA-15-uncal(100), (b) NR/SBA-15-cal(100), (c) NR/MCM-41-uncal(100), and (d) NR/MCM-41-cal(100) (at 150 magnification).

4.2.3 Textural Properties of NR Composites

4.2.3.1 Influence of Preparation Techniques

Two-roll mill produced NR composite sheet; whereas, slurry technique generated thin film of NR composite. From this different appearance of NR composite, textural properties of NR composite prepared by each technique were also investigated.

(A)	Textural	Properties	of	NR	Composite Prepared by Two-roll Mill Mixing

In Table 4.5, the textural properties of NR sheet and NR/Si1 composite (NR/Si1(5)) with silica content of 5 phr prepared by two-roll mill mixing are summarized. In comparison with NR sheet, BET surface area and average pore volume of this NR composite were 4 m^2 g^{-1} and 0.001 cm^3 g^{-1}, respectively that were lower but average pore size (87.4 Å) was higher. These results may be ascribed to chopping and pasting steps of NR among mixing process. Since, NR filled with silica reinforcing material was chopped and pasted on roll to improve distribution of silica material in NR. Both steps might be effect on decreasing porosity of prepared NR composite. Moreover, inter particle pore on surface of NR composite might cause to increase its average pore size (D_p) when compared to NR. Therefore, these results were ensured that two-roll mill mixing was unable technique to increase NR porosity.

Table 4.5 Textural Properties of NR Composite Prepared by Two-roll mill Mixing

Sample	S_{BET}[a](m^2 g^{-1})	V_P[b](cm^3 g^{-1})	D_p[c](Å)
NR[d]	19	0.003	42.2
NR/Si1(5)	4	0.001	87.4

[a] BET surface area.

[b] Average pore volume.

[c] Average pore size.

[d] Natural rubber.

(B) Textural Properties of NR Composites
Prepared by Slurry Technique

The textural properties of NR film and NR/Si1 composite (NR/Si1(200)) with contents of 200 phr prepared by slurry technique are summarized in Table 4.6. It shows that BET surface area, average pore volume and average pore size of this NR composite as 166 m^2 g^{-1}, 0.313 cm^3 g^{-1} and 58.2 Å, respectively were higher than that of NR film as 7 m^2 g^{-1}, 0.003 cm^3 g^{-1} and 41.2 Å, severally. On the other hand, in comparison with the silica material (Si1), BET surface area and average pore volume of this NR composite were lower. It might be ascribed to some part of silica surface covered by NR in red marked. As shown in Figure 4.12, It was also seen that some silica particle was beetle from NR surface and then built interparticle pore. This might be cause to increase its average pore size when compared with silica material. These results indicated that porosity of NR composite was higher than that of NR film; nevertheless, it was lower than that of silica material. Therefore, slurry technique was appropriate preparation of NR composite to increase NR porosity.

Table 4.6 Textural properties of NR Composites Prepared by Slurry Technique

Sample	$S_{BET}{}^a$(m^2 g^{-1})	$V_P{}^b$(cm^3 g^{-1})	$D_p{}^c$(Å)
NR^d	7	0.003	41.2
Si1	468	0.677	45.9
NR/Si1(200)	166	0.313	58.2

[a] BET surface area.

[b] Average pore volume.

[c] Average pore size.

[d] Natural rubber.

4.2.3.2 Textural Properties of NR/Silica Gel Composites

(A) Influence of Particle Sizes of Silica Gel

Table 4.7 shows textural properties of NR composite filled with different sizes of silica gels (Si1-Si4). It revealed that BET surface area, average pore volume and average pore size of NR composite filled with the smallest size of silica gel (Si4) that were 192 m^2 g^{-1}, 0.348 cm^3 g^{-1} and 62.3 Å, respectively were higher than that of NR composite filled with other larger sizes such as Si3, Si2 and Si1. These results can be ascribed that in equal weight, amount of smaller particle size of silica gel was more than that of larger size one that it can more overlap. Then, the smaller particle size of silica gel can increasingly beetle from NR surface. It might increase porosity of NR composite filled with smaller particle size of silica gel. This confirms that porosity of NR composite increased with decreasing size of silica material filled in NR composite.

Table 4.7 Influence of Particle Sizes of Silica Gels on Textural Properties of NR
Composites Prepared by Slurry Technique

Sample	$S_{BET}{}^a$ (m^2 g^{-1})	$V_P{}^b$ (cm^3 g^{-1})	$D_P{}^c$ (Å)
NR^d	7	0.003	41.2
NR/Si1(200)	166	0.313	58.2
NR/Si2(200)	163	0.333	58.1
NR/Si3(200)	161	0.343	57.2
NR/Si4(200)	192	0.348	62.3

[a] BET surface area.

[b] Average pore volume.

[c] Average pore size.

[d] Natural rubber.

(B) Influence of Silica Gel Contents

The effect of contents of silica gel filled in NR composite on textural properties of resulting NR composite was investigated. As shown in Table 4.8, BET surface area and average pore volume of NR composite with the most loading of silica gel (NR/Si4(300)) that were 194 m^2 g^{-1} and 0.405 cm^3 g^{-1}, respectively were higher than that of NR/Si4 composites with lower contents of silica gel. It might be ascribed that silica gel with higher content can increasingly thread from NR surface. However, average pore size of NR/Si4(300) was less than that of NR/Si4 composites with lower contents of silica gel; since, silica particle with higher content can be close together more than silica gel with lower contents as shown in Figure 4.13 (a), (b) and (c). These results can suggest that BET surface area and average pore volume of NR composite increased while average pore size decreased with increasing silica gel content in NR composite.

Table 4.8 Influence of Silica Gel Contents on Textural Properties of NR

Composites Prepared by Slurry Technique

Sample	S_{BET}^a(m^2 g^{-1})	V_P^b(cm^3 g^{-1})	D_P^c(Å)
NR[d]	7	0.003	41.2
NR/Si4(100)	101	0.220	63.2
NR/Si4(200)	192	0.348	62.3
NR/Si4(300)	194	0.405	60.4

[a] BET surface area.

[b] Average pore volume.

[c] Average pore size.

[d] Natural rubber.

.

4.2.3.3 Textural Properties of NR/Mesoporous Silica Composites

(A) Influence of Mesoporous Silica Types

Textural properties of NR composite filled with each type of mesoporous silicas were investigated as shown in Table 4.9. It was found that BET surface area and average pore volume of NR/MCM-41-cal(150) as 235 m^2 g^{-1} and 0.250 cm^3 g^{-1}, respectively were higher than that of NR/SBA-15-cal composite with equal content of silica material as 81 m^2 g^{-1} and 0.183 cm^3 g^{-1}, respectively. Then, MCM-41 showed a larger specific surface area compared to SBA-15 (Yang, 2003). Moreover, average pore size of NR/MCM-41-cal(150) as 24.8 Å was lower than that of NR/SBA-15-cal(150) as 71.5 Å. This indicated that higher porosity of mesoporous silica resulting in higher porosity of NR composite filled this silica.

(B) Influence of Mesoporous Silica Contents

The effect of contents of mesoporous silicas on textural properties of resulting NR composite were investigated as revealed in Table 4.9. It can be still seen that BET surface area, average pore volume and average pore size of NR/MCM-41-cal(150) as 235 m^2 g^{-1}, 0.250 cm^3 g^{-1} and 24.8 Å, respectively were higher than that of NR composite filled with this type of silica material with lower content as 100 phr. Similar result was found in NR composite filled with SBA-15. Then, it indicated that porosity of NR composite increased with increasing mesoporous silica (both MCM41-cal and SBA15-cal) content in NR composite.

Table 4.9 Influence of Mesoporous Silica Contents on Textural Properties of NR
Composites Prepared by Slurry Technique

Sample	S_{BET}^{a}(m^2 g^{-1})	V_P^{b}(cm^3 g^{-1})	D_p^{c}(Å)
NR^d	7	0.003	41.2
NR/MCM41-cal^e(100)	185	0.175	22.6
NR/MCM41-cal^e(150)	235	0.250	24.8
NR/SBA15-cal^e(100)	53	0.114	70.9
NR/SBA15-cal^e(150)	81	0.183	71.5

^{a} BET surface area.

^{b} Average pore volume.

^{c} Average pore size.

^{d} Natural rubber.

^{e} Calcined mesoporous silica.

(C) Influence of Calcination of Mesoporous Silicas

Textural properties of NR composite filled with calcined and uncalcined mesoporous silica were investigated. As reported in Table 4.10, it was found that BET surface area and average pore volume of NR/MCM-41-uncal(100) as 1 m^2 g^{-1} and 0.002 cm^3 g^{-1}, respectively were much lower than that of NR/MCM-41-cal(100) as 185 m^2 g^{-1} and 0.175 cm^3 g^{-1}, respectively. While its average pore size as 78.4 Å was patently higher when compared to NR/MCM-41-cal(100) as 22.6 Å. A similar result, where filling of SBA-15-uncal into NR composite gave lower BET surface area, average pore volume but higher average pore size of resulting NR composite in comparison with NR/SBA-15-cal composite. These results were ascribed to calcination of mesoporous silica to get rid of template molecule that can increase porosity of this silica material (Berube and Kaliaguine, 2008). Then, it might be able to increase porosity of NR composite filled with calcined mesoporous silica. This also indicated that NR/uncalcined mesoporous silicas composites have absolutely low porosity.

Table 4.10 Influence of Template Molecules on Textural Properties of NR
Composites Prepared by Slurry Technique

Sample	$S_{BET}{}^a(m^2\ g^{-1})$	$V_P{}^b(cm^3\ g^{-1})$	$D_p{}^c(\mathring{A})$
NR[d]	7	0.003	41.2
NR/MCM41-uncal[e](100)	1	0.002	78.4
NR/MCM41-cal[f](100)	185	0.175	22.6
NR/SBA15-uncal[e](100)	8	0.016	79.5
NR/SBA15-cal[f](100)	53	0.114	70.9

[a] BET surface area.

[b] Average pore volume.

[c] Average pore size.

[d] Natural rubber.

[e] Uncalcined mesoporous silica.

[f] Calcined mesoporous silica.

4.2.4 Silica Contents of NR Composites Prepared by Slurry Technique

To confirm silica materials contents in prepared NR composite, thermal degradation characteristics of NR composites was studied. Thermogravimetric analysis (TGA), which was carried out on a Perkin Elmer Pyris Diamond Thermogravimeter (TG/DTA) under dry air flow, was done on NR composite in order to determine the content of silica material in this composite.

4.2.4.1 Apparent Content of Silica Materials

From the thermogravimetric analysis, Figure 4.15 reveals weight loss (TG) and differential weight loss (DTG) curves of NR/Si1(200). It shows several stages of thermal decompositions. The first stage occurred around 100 °C due to dehydration, meaning the removal of physisorbed water from the surface of the silica particles. Then degradation of NR molecular chains took place around 300 °C as second stage and completed at 450 °C (Martins *et al.*, 2008). This was a major weight loss with a maximum of the DTG peak at 300 °C corresponding to 33.44% weight

loss of NR; on the other hand, it implied that there was 66.56% of silica content remaining of 199.67 phr. In this major weight loss, it also showed small weight loss of dehydroxylation due to the condensation of the OH groups in the silica particles (Jong *et al.*, 2009) around 350 °C. Finally, the weight loss around 450 to 600 °C was derived from decomposition of carbonaceous residues from NR (Martins *et al.*, 2008). The characteristic of silica material contents in other studied NR composites are summarized in Table 4.11. Interestingly, these results reveal that apparent contents of silica material in each NR composite were close to theoretical contents. From thermal degradation characteristics and textural properties of NR composite prepared by slurry technique, it was strongly suggested that slurry technique was proper to prepare NR composite.
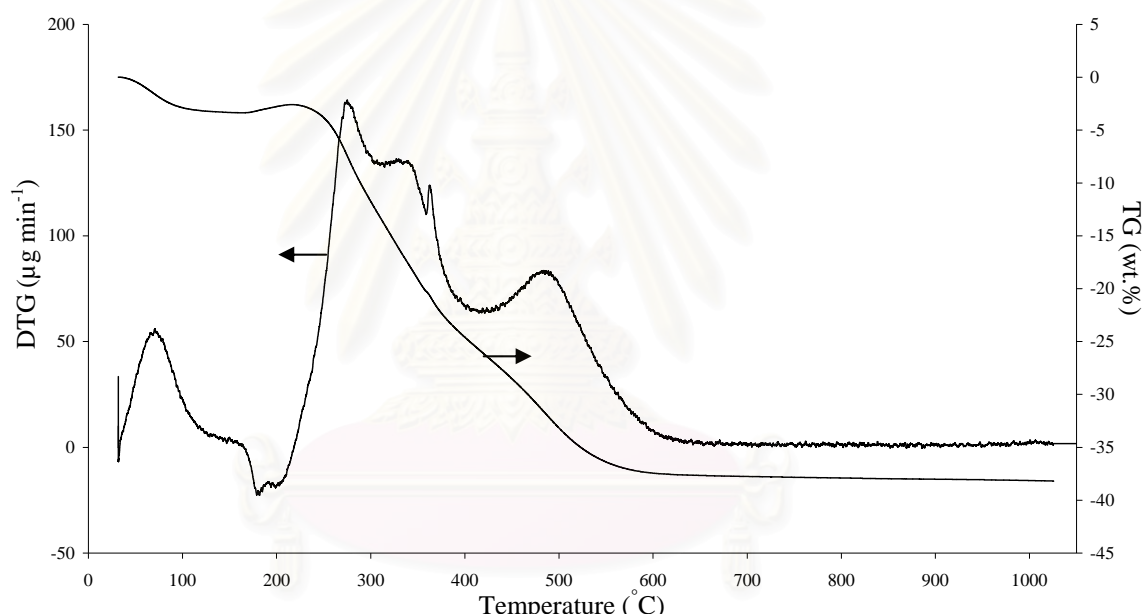
Figure 4.15 Weight loss (TG) and differential weight loss (DTG) curves of NR/Si1(200).

Table 4.11 Theoretical and Apparent Contents of Silica Materials in NR Composites

Sample	weight loss (wt.%)		silica material contents (wt.%)		Apparent silica content (phr)[a]
	Theoretical	Apparent	Theoretical	Apparent	
NR/Si1(200)	33.33	33.44	66.67	66.56	199.67
NR/Si4(200)	33.33	34.08	66.67	65.92	197.75
NR/Si4-TS(200)	38.36[b]	36.10	66.67	68.93[c]	206.78
NR/Si4(300)	25.00	26.88	75.00	73.12	292.48
NR/MCM41-cal(100)	50.00	57.70	50.00	42.30	84.60
NR/MCM41-uncal(100)	68.93[d]	65.30	50.00	53.63[e]	107.26

[a] Part per hundred part of rubber.

[b] Including weight of organosilane as 5.03 wt.%.

[c] Weight percentage of totality of silica material and organosilane.

[d] Including weight of organic template as 18.93 wt.%.

[e] Weight percentage of totality of silica material and organic template.

4.3 Study of N_2 Adsorption-desorption Isotherms of Silica Materials and NR composites

For NR composite filled with silica gel, the N_2 adsorption–desorption isotherms of NR, silica gel (Si4) and NR/Si4 composite (NR/Si4(300)) with silica content of 300 phr are illustrated in Figure 4.16. The N_2 adsorption–desorption isotherm of NR showed absolutely low quantity adsorbed. It implied that NR was non-porous adsorbent or has less porosity. Besides, as mentioned in the section of textural properties of pure silica gel, it indicated that the isotherm of NR/Si4(300) was identical with that of Si4. Hence, it implied that porosity of NR composite consisted of silica gel was influenced from silica gel. But the quantity adsorbed of NR/Si4(300) was less than that of Si4, this result caused BET surface area of NR composite filled with silica gel lower than one of silica gel as shown in Table 4.7 and 4.1, respectively.

For N_2 adsorption–desorption isotherms of NR composites filled with mesoporous silicas, both MCM-41 and SBA-15, Figure 4.17 shows the N_2 adsorption–desorption isotherms of NR, MCM-41-cal, NR/MCM-41-cal, MCM-41-uncal and NR/MCM-41-uncal. As mentioned in the section of textural properties of calcined and uncalcined MCM-41, it could indicate that the isotherms of NR

composites filled with those of MCM-41 were absolutely different from NR and their silica particles filled in NR composite. Moreover, the adsorption quantities of both NR composites were less than that of filled particles. Especially, the adsorption quantity of NR/MCM-41-uncal was slight. These results caused BET surface areas of both NR composites lower than one of each its particle as shown in Table 4.1 and 4.10, respectively. Furthermore, hysteresis loop of both composites occurred at higher P/P_0 when compared to that of filled particles. It implied that pore size of these NR/MCM-41 composites were higher than that of each filled particles. These larger pores may be interparticle pore.

Figure 4.18 shows the N_2 adsorption–desorption isotherms of NR, SBA-15-cal, NR/SBA-15-cal, SBA-15-uncal and NR/SBA-15-uncal. As mentioned in the section of textural properties of pure SBA-15, it reveals that the isotherms of both NR composites filled with calcined SBA-15 and uncalcined SBA-15, it was found that the quantity adsorbed of both NR composites were less than that of each their particles. Particularly, the quantity adsorbed of NR/SBA-15-uncal was slight. These results caused BET surface areas of both NR composites lower than one of each its particle as shown in Table 4.1 and 4.10, respectively. In addition, the hysteresis loop of NR/SBA-15-uncal occurred at P/P_0 higher than that its particle. This indicated that pore size of this NR composite was higher than that of its particle, and this pore with larger size may be new occurrence interparticle pore. However, the isotherm of NR/SBA-15-cal was similar to one of its particle, and their hysteresis loops occurred at approximate P/P_0. It may indicate that porosity of NR/SBA-15-cal was influenced from particle over NR.
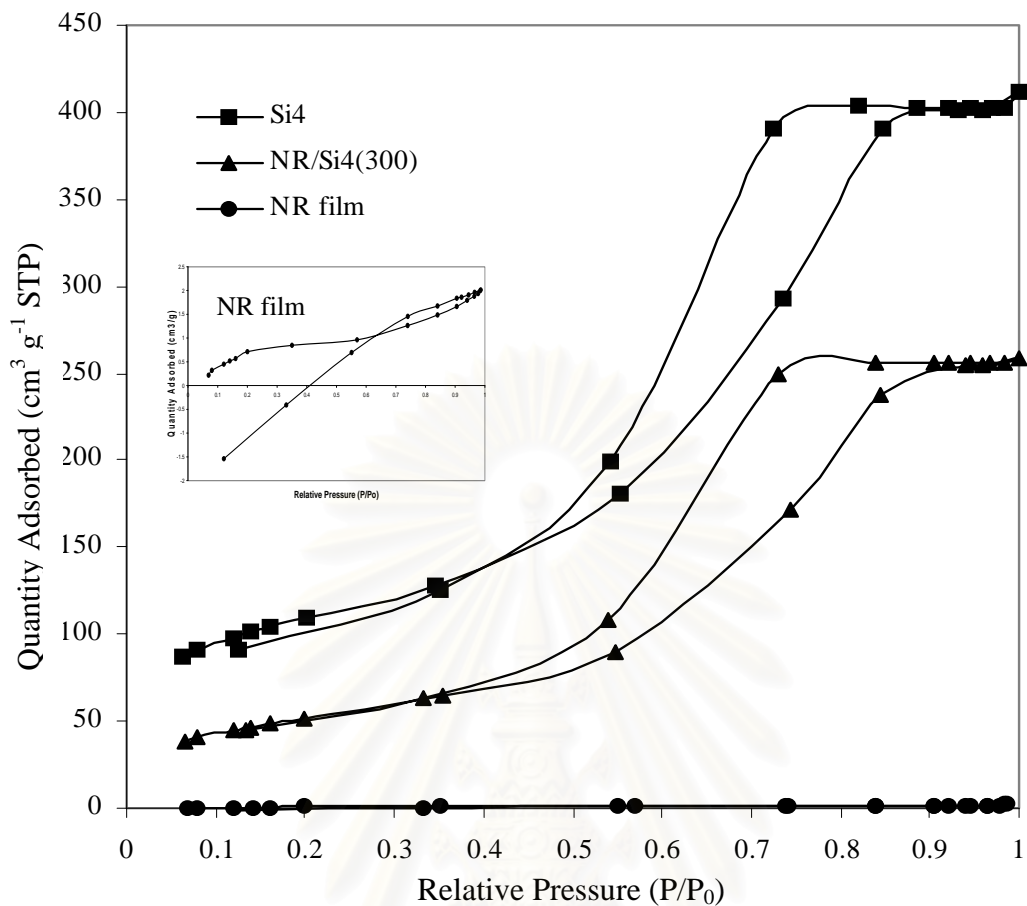
Figure 4.16 N_2 adsorption-desorption isotherms of NR, Si4 and NR/Si4(300).

สถาบันวิทยบริการ

จุฬาลงกรณ์มหาวิทยาลัย
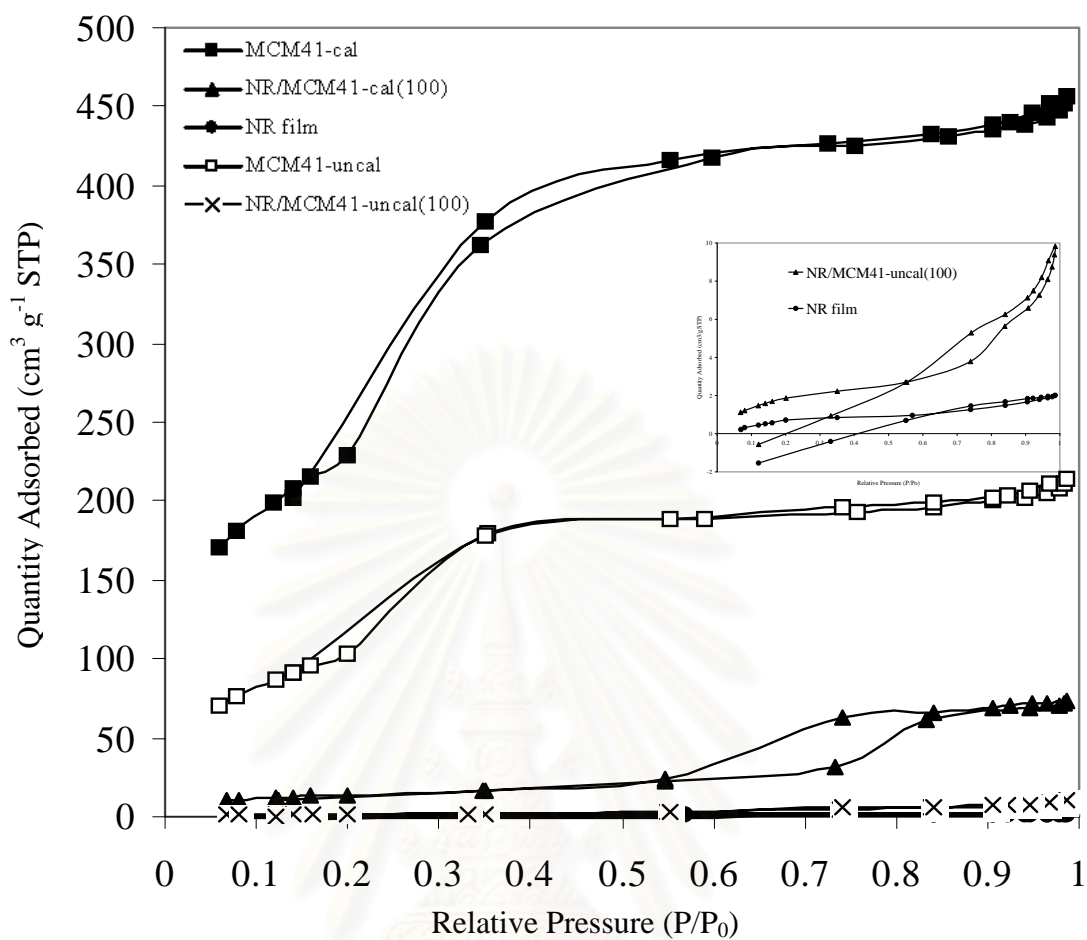
Figure 4.17 N$_2$ adsorption-desorption isotherms of NR, MCM-41-cal, NR/MCM-41-cal(100), MCM-41-uncal, and NR/MCM-41-uncal(100).
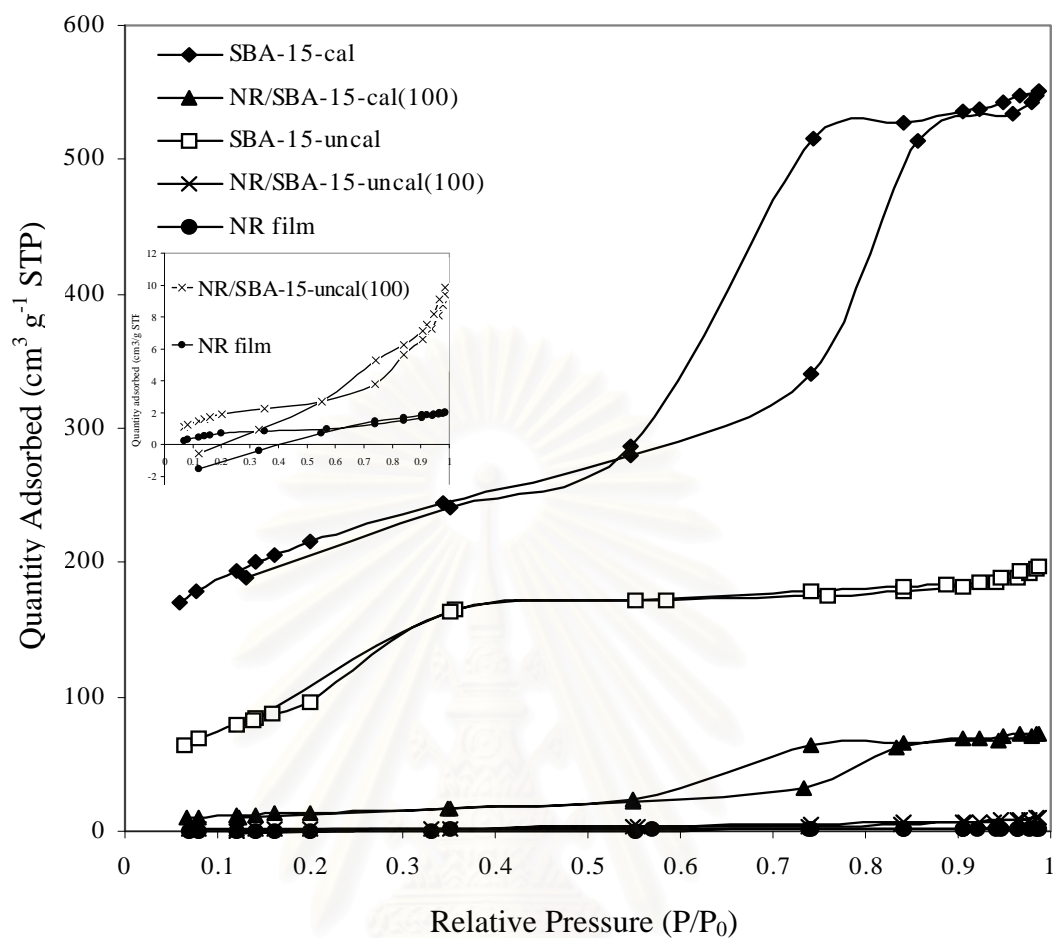
Figure 4.18 N_2 adsorption-desorption isotherms of NR, SBA-15-cal, NR/SBA-15-cal(100), SBA-15-uncal and NR/SBA-15-uncal(100).

4.4 Study of NR Composites in Ascorbic Acid Adsorption and Desorption

The measurement of amount of ascorbic acid adsorbed and desorbed of NR composite was investigated by UV/Vis spectrophotometry technique on a V-530 UV/VIS Spectrophotometer.

To compare adsorption capability of NR composite with silica material, NR composite and its silica material were taken to adsorb 15 ml of 3.4×10^{-4}M of ascorbic acid for 1 h at ambient temperature. Afterwards, amount of adsorbed ascorbic acid was measured by UV/Vis spectrophotometry technique.

Amount of adsorbed ascorbic acid per weight of adsorbent such as MCM41-uncal and NR/MCM41-uncal composite (NR/MCM41-uncal(100)) with silica content of 100 phr are summarized in Table 4.12. In comparison with particle, amount of adsorbed ascorbic acid on this NR composite was lower; as, it may be effect from lower BET surface area of NR/MCM41-uncal as shown in Tables 4.1 and 4.10, respectively. This result confirmed that silica material can adsorb ascorbic acid more than NR composite filled with this silica material, in equal weight of silica material.

Table 4.12 Amount of Ascorbic Acid Adsorption[a] on Adsorbent

Adsorbent	S_{BET}[b] ($m^2\ g^{-1}$)	V_p[c] ($cm^3\ g^{-1}$)	Absorbance	Amount of adsorbed AA[d] ($\times 10^{-4}$ mole $g^{-1}_{adsorbent}$)
MCM41-uncal[e]	398	0.363	2.3532	4.454
NR/MCM41-uncal[e](100)	1	0.002	3.2085	0.165

[a] Adsorption condition: adsorb 15 mL of 3.4×10^{-4} M of ascorbic acid for 1 h at ambient temperature.

[b] BET surface area.

[c] Average pore volume.

[d] Ascorbic acid.

[e] Uncalcined mesoporous silica.

4.4.1 Influence of Particle Sizes of Silica Gel

The firstly studied parameter was particle size of silica material. As shown in Table 4.13, it can be seen that decreasing silica size filled in NR composite caused to increase adsorption and desorption of ascorbic acid on NR composite. BET surface area of NR composite consisted of smaller size of silica particle (Si4) was higher than that of composite consisted of larger size of silica particle (Si1).

Table 4.13 Influence of Particle Sizes of Silica Gel in Ascorbic Acid Adsorption and Desorption[a] of NR Composites

Adsorbent	S_{BET}[b] ($m^2 g^{-1}$)	V_p[c] ($cm^3 g^{-1}$)	Absorbance	Amount of desorbed AA[d] ($x10^{-4}$ mole $g^{-1}_{adsorbent}$)
NR	7	0.003	0.2971	0.032
NR/Si1[e](200)	166	0.313	0.6510	0.458
NR/Si4[f](200)	192	0.348	0.8715	0.771

[a] Adsorption condition: adsorb 40 mL of 1.13 x 10^{-2}M of ascorbic acid for 15 min at ambient temperature.

Desorption condition: desorb 50 mL of 3.16 x 10^{-3}M of sodiumthiosulphate aqueous solution for 15 min at ambient temperature.

[b] BET surface area.

[c] Average pore volume.

[d] Ascorbic acid.

[e] Size of silica gel: 149-210 µm.

[f] Size of silica gel: 63-74 µm.

4.4.2 Influence of Silica Material Contents

Contents of silica material were also observed. As shown in Table 4.14, it reveals that increasing silica gel contents in NR composite caused to increase ascorbic acid adsorption and desorption; because, BET surface area and average pore volume of NR composite increased with increasing content of silica gel in NR composite as shown in Table 4.14. This reason implied that ascorbic acid adsorption and desorption of NR composite increased with increasing its BET surface area and average pore volume.

Table 4.14 Influence of Silica Material Contents in Ascorbic Acid Adsorption and Desorption[a] of NR Composites

Adsorbent	S_{BET}[b] $(m^2 g^{-1})$	V_p[c] $(cm^3 g^{-1})$	Absorbance	Amount of desorbed AA[d] $(x10^{-4}$ mole $g^{-1}_{adsorbent})$
NR	7	0.003	0.2971	0.032
NR/Si4(100)	101	0.220	0.6236	0.635
NR/Si4(200)	192	0.348	0.8715	0.771
NR/Si4(300)	194	0.405	1.0783	0.890

[a] Adsorption condition: adsorb 40 mL of 1.13 x 10^{-2}M of ascorbic acid for 15 min at ambient temperature.

Desorption condition: desorb 50 mL of 3.16 x 10^{-3}M of sodiumthiosulphate aqueous solution for 15 min at ambient temperature.

[b] BET surface area.

[c] Average pore volume.

[d] Ascorbic acid.

4.4.3 Influence of Surface Functionalization of Silica Materials

Influence of functionalizations of silica material on adsorption and desorption capability of NR composites were also investigated. As shown in Table 4.15, it was found that amount of adsorption and desorption of ascorbic acid of NR composites consisted of functionalized silica materials were lower, in comparison with NR composite filled with unmodified material. It might suggest that decreasing of porosity of functionalized silica materials due to covering of organosilane on porous surface of silica might cause to decrease porosity of NR composite filled with this particle and then also decrease amount of adsorbed and desorbed ascorbic acid of NR composite.

Table 4.15 Influence of Surface Functionalization of Silica Materials in Ascorbic
Acid Adsorption and Desorption[a] of NR Composites

Adsorbent	Absorbance	Amount of desorbed AA[b] $(\times 10^{-4} \text{ mole g}^{-1}_{\text{adsorbent}})$
NR	0.2971	0.032
NR/Si4(300)	1.0783	0.890
NR/Si4-TS[c](300)	0.5340	0.245
NR/Si4-PS[d](300)	0.4449	0.156

[a] Adsorption condition: adsorb 40 mL of 1.13×10^{-2}M of ascorbic acid for 15 min at ambient temperature.

 Desorption condition: desorb 50 mL of 3.16×10^{-3}M of sodiumthiosulphate aqueous solution for 15 min at ambient temperature.

[b] Ascorbic acid.

[c] Si4 functionalized by trimethylsilylation.

[d] Si4 functionalized by propylsilylation.

4.4.4 Influence of Vulcanization of NR Composite

To improve stability of resulting NR composite, NR composite was vulcanized by vulcanizing agent such as sulfur 2 phr, ZnO 5 phr, stearic acid 1.5 phr and MBTS 1 phr (Suda and Kornteenee, 2004) at the same condition of preparation of NR composite by slurry technique. Table 4.16 shows comparison of amount of ascorbic acid adsorption and desorption of vulcanizated and unvulcanizetd NR composite. It was found that amount of ascorbic acid adsorption and desorption of vulcanizated NR composite was lower. It may be ascribed to covering of vulcanizing agents on porosity of NR composite. This indicated that vulcanization might reduce BET surface area and adsorption and desorption properties of resulting NR composite.

Table 4.16 Influence of Vulcanization on Adsorption and Desorption[a] of Ascorbic Acid of NR/Silica Gel Composites

Adsorbent	Absorbance	Amount of desorbed AA[b] $(x10^{-4}$ mole $g^{-1}_{adsorbent})$
NR	0.2971	0.032
NR/Si4(300)	1.0783	0.890
NR/Si4(300)-v[c]	0.5942	0.289

[a] Adsorption condition: adsorb 40 mL of 1.13 x 10^{-2}M of ascorbic acid for 15 min at ambient temperature.

  Desorption condition: desorb 50 mL of 3.16 x 10^{-3}M of sodiumthiosulphate aqueous solution for 15 min at ambient temperature.

[b] Ascorbic acid.

[c] Vulcanizated NR composite: vulcanizing agents such as sulfur 3 phr, ZnO 5 phr, stearic acid 2 phr and MBTS 1.8 phr (Suda, 2004) at same condition of preparation of NR composite by slurry technique.

4.4.5 Influence of Calcination of Mesoporous Silica

Table 4.17 shows comparison of amount of ascorbic acid adsorption and desorption between NR composite filled calcined and uncalcined mesoporous silica. It was found that NR/uncalcined mesoporous silica composite had higher amount of ascorbic acid adsorption and desorption than that of NR/calcined mesoporous silica composite; though, its BET surface area and average pore volume were lower as shown in Table 4.17. It indicated that both BET surface area and average pore volume of NR/mesoporous silica composites were unable to account for their adsorption and desorption capability. Interestingly, it was observed that interparticle pore might be able to increase adsorption and desorption ascorbic acid capability. From higher amount of ascorbic acid adsorption and desorption of NR/uncalcined mesoporous silica composites, it might suggest that its porosity analyzed by N_2 adsorption-desorption analyzer might not be exact; as, its porosity might not be in detectable porous range of this analyzer; since, size of interparticle pore might be over the analyzer limitation.

Table 4.17 Adsorption and Desorption[a] of Ascorbic Acid on various NR/Mesoporous Silica Composites

Adsorbent	S_{BET}[b] $(m^2 g^{-1})$	V_p[c] $(cm^3 g^{-1})$	Absorbance	Amount of desorbed AA[d] $(x10^{-4}$ mole $g^{-1}_{adsorbent})$
NR	7	0.003	0.2971	0.032
NR/MCM41-cal[e](100)	185	0.175	1.0038	1.469
NR/SBA15-cal[e](100)	53	0.114	0.4850	0.410
NR/MCM41-uncal[f](100)	1	0.002	2.0030	3.483
NR/SBA15-uncal[f](100)	8	0.016	0.7915	1.021

[a] Adsorption condition: adsorb 40 mL of 1.13 x 10^{-2}M of ascorbic acid for 15 min at ambient temperature.

Desorption condition: desorb 50 mL of 3.16 x 10^{-3}M of sodiumthiosulphate aqueous solution for 15 min at ambient temperature.

[b] BET surface area.

[c] Average pore volume.

[d] Ascorbic acid.

[e] Calcined mesoporous silica., [f] Uncalcined mesoporous silica.

4.4.6 Influence of Initial Concentration of Ascorbic Acid

As, both BET surface area and average pore volume of NR/mesoporous silica composites were unable to account for adsorption and desorption capability of these composites. Moreover, interparticle pore might be able to increase adsorption and desorption ascorbic acid capability. Then to prove this assumption, it was also desired to study liquid phase adsorption isotherm, but concentration of ascorbic acid at equilibrium condition cannot be detected due to limitation of UV/Vis spectrophotometer. Lastly, influence of initial concentrations of ascorbic acid as 0.1, 0.2, 0.4, 0.6, 0.8, 1.0, 1.2, and 1.4 %w/v on amount of desorbed ascorbic acid were instead investigated. From UV/Vis absorption analysis, all results revealed in graphical form i.e., Figure 4.19 shown adsorption and desorption capability of ascorbic acid on NR/MCM-41-cal at loading range 50 to 100 phr. It shows that amount of ascorbic acid adsorption and desorption of NR composite increased with increasing initial concentration of ascorbic acid. As a result, it can suggest that type of adsorption was physisorption; as, it was not site to site adsorption. Moreover, the accumulation of ascorbic acid molecule on adsorbent surface increased with increasing initial concentration of ascorbic acid, similar to result of NR composite filled with other types of silica materials as shown in Figure 4.20 to Figure 4.22. Therefore, it was possible that NR composite filled with mesoporous silica with lower BET surface area and average pore volume had higher amount of adsorbed and desorbed ascorbic acid due to higher adsorption site from higher pore size.
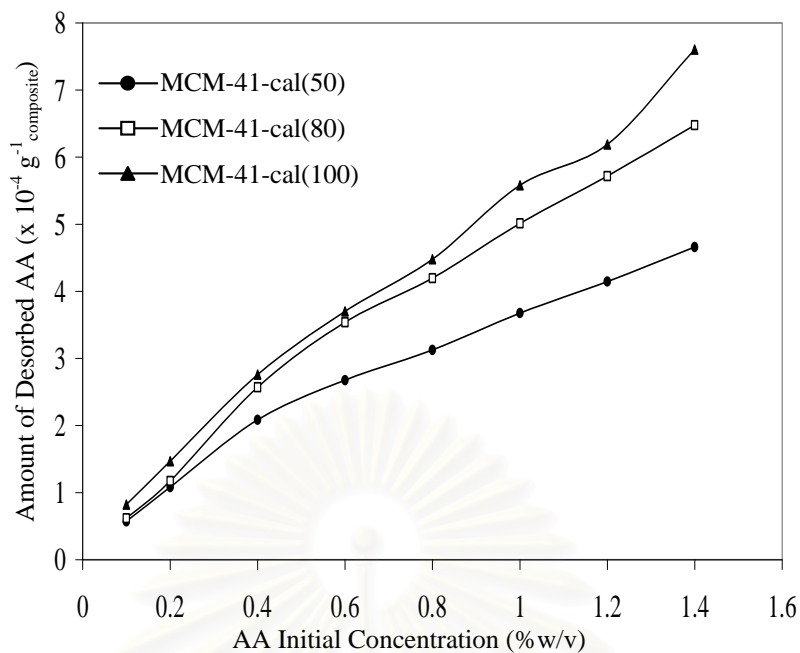
Figure 4.19 Dependence of amount of desorbed AA from NR/MCM-41-cal
composite on AA initial concentration.
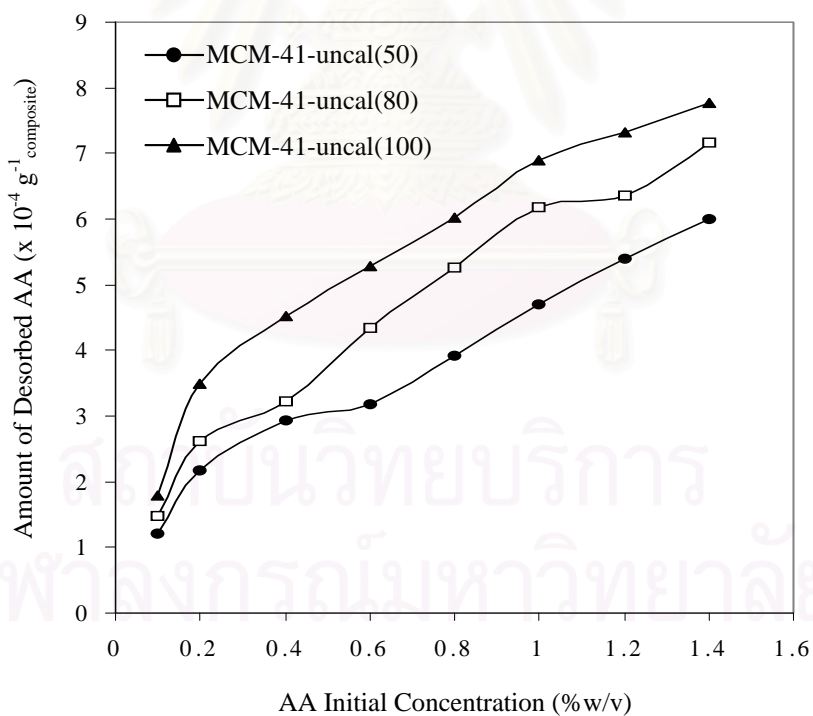
Figure 4.20 Dependence of amount of desorbed AA from NR/MCM-41-uncal
composite on AA initial concentration.
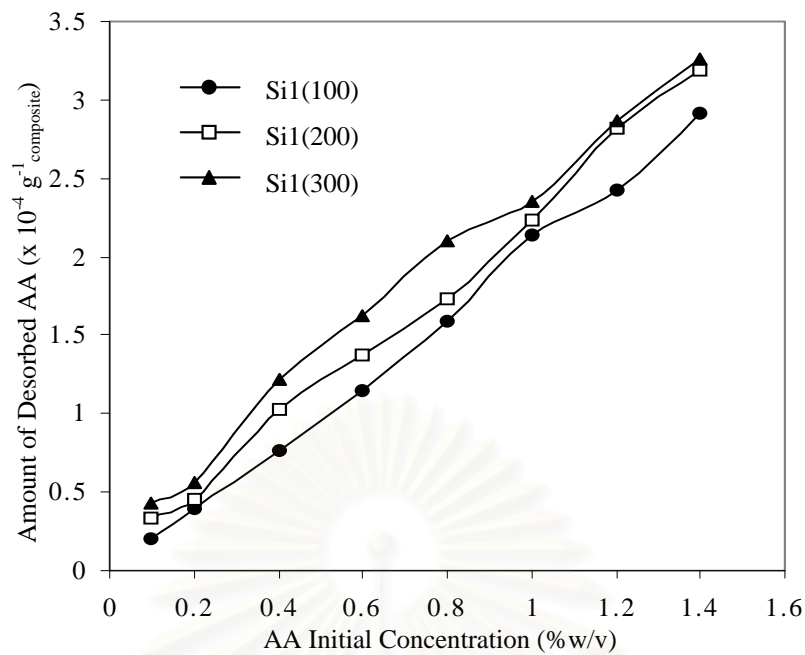
Figure 4.21 Dependence of amount of desorbed AA from NR/Si1 composite on AA
initial concentration.
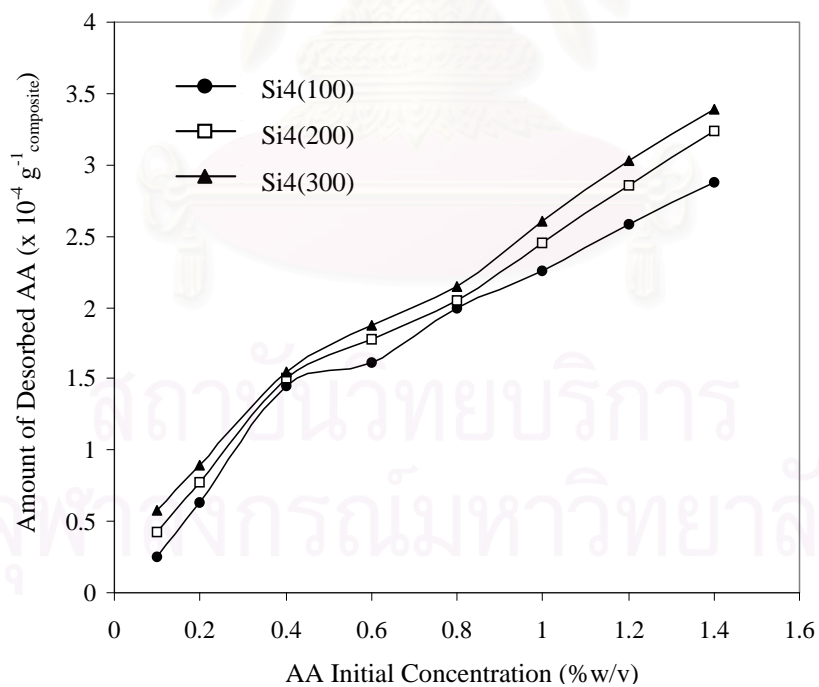
Figure 4.22 Dependence of amount of desorbed AA from Si4 composite on AA
initial concentration.

CHAPTER V

CONCLUSION AND RECOMMENDATIONS

5.1 Conclusion

Trimethysilylation and propylsilylation can modify functional group on surface of silica material; nevertheless, it resulted in decreasing porosity of functionalized particle.

Slurry technique was appropriate preparation of porous NR composite. Besides, analyzed loading content of silica particle was close to calculated content.

Porosity of resulting NR composite increased with increasing content and decreasing size of silica material. At equal loading of silica material, porosity of NR/MCM-41-cal was the highest when compared to other type of studied silica materials. Moreover, calcination of mesoporous silica can increase BET surface area and average pore volume of NR/calcined mesopous silica composites.

High BET surface area and average pore volume of NR composites affect high adsorption and desorption of ascorbic acid, except for NR/mesoporous silica composites. High adsorption and desorption of ascorbic acid of NR/mesoporous silica composites might be from high interparticle pore size. Besides surface functionalization of silica material and vulcanization of resulting composite resulted in reducing amount of ascorbic acid adsorption and desorption of resulting composite. Moreover, amount of ascorbic acid adsorption and desorption of NR composite increased with increasing initial concentration of ascorbic acid.

5.2 Recommendations

Except for vitamic C (ascorbic acid), vitamin A (retinyl acetate) and vitamin E (α-tocopherol) were also good for skin health. Then, the other applications of these NR composites such as adsorption of vitamin A and vitamin E were interesting to further study.

REFERENCES

Araujo, A.S. and Jaroniec, M. Thermogravimetric monitoring of the MCM-41 synthesis. Thermochim. Acta. 363 (2000): 175-180.

Arunyanad, P. Adsorption of gaseous fuel on natural rubber surface. Master's Thesis, Department of Chemical Technology, Faculty of Science, Chulalongkorn University, 2005.

Avelino, C., Qiubin, K., Maria, T. N. Synthesis of MCM-41 with different pore diameter without addition of auxiliary organics. Chem. Mater. 9 (1997): 2123-2126.

Berube, F. and Kaliaguine, S. Calcination and thermal degradation mechanisms of triblock copolymer template in SBA-15 materials. Micropor. Mesopor. Mater. 115 (2008): 469–479.

Blow, C.M. Reinforcement of elastomers. London: Newnes-Butter worths, 1980.

Blow, C.M. Rubber technology and manufacture. England: Page Bros, 1982.

Brydson, J.A. Rubber chemistry. London: Applied Science, 1978.

Chantippimarn, S. Composite material from natural rubber and sticky rice flour. Master's Thesis, Program of Petrochemical and Polymer Science, Faculty of Science, Chulalongkorn University, 2001.

Elizabeth, A. T., Harald, R., Dieter, F., Yining H., and John, F. C. Characterization of ZnE (E = S, Se, or Te) materials synthesized using silylated chalcogen reagents in mesoporous MCM-41. J. Phys. Chem. B. 110 (2006): 16261-16269.

Hu, L., JI, S., Jiange, Z., Son, H., Wu, P., Liu, Q. Direct synthesis and structural characteristics of ordered SBA-15 mesoporous silica containing tungsten oxides and tungsten carbides. J. Phys. Chem. C. 111 (2007): 15173-15184.

Imperor-Clerc, M., Davidson, P. and Davidson, A. Existence of a microporous of silica-based SBA-15 materials templated by triblock copolymer. J. Am. Chem. Soc. 122 (2000): 11925-11933.

Jong, M. K., Sang, M. C., Sung, M. K., Kyo, S. K., Jinsoo, K., Woo, S. K. Control of hydroxyl group content in silica particle synthesized by the sol-precipitation process Ceram. Int. 35 (2009): 1015–1019.

Jones, R.M. Mechanics of composite materials. Washington D.C.: Scripta book, 1975.

Kierys, A., Pasieczna, S., Ryczkowski, J., and Goworek, J. Thermal stability of chemically bonded phases on silica gel by photoacoustic FT-IR spectroscopy. J. Phys. IV France. 137 (2006): 291-295.

Koyano, K. A., Tatsumi, T., Tanaka, Y., and Nakata, S. Stabilization of mesoporous molecular sieves by trimethylsilylation. J. Phys. Chem. 101 (1997): 9436-9440.

Kwakye, J. K. The use of stabilizers in the uv assay of ascorbic acid. J.Talanta. 51 (2000): 197–200.

Lewin, S. Vitamin c: Its molecular biology and medical potential. London: Academic, 1976.

Li, J., Shi, J., Dong, Z., Qian, S., and Wei, C. Diazobenzene chromophore-doped silica films with large two-photon absorption cross-section. Dyes Pigments. 82 (2009): 204-208.

Mark, J.E., Abou-Hussein, R., Sen, T.Z., and Kloczkowski, A. Some simulation on filler reinforcement in elastomer. Polymer. 46 (2005): 8894-8904.

Martins, M. A., Moreno, R.M.B., McMahan, C. M., Brichta, J. L., Goncalves, P. S., Mattoso, L.H.C. Thermooxidative study of raw natural rubber from Brazilian IAC 300 series clones. Thermochim. Acta. 474 (2008): 62-66.

Morton, M. Rubber technology. 2nd ed. New York: Van Nostrand Reinhold, 1973.

Oscar A. A., Andrea R. B., Maria L. M., and Lizandra L. B. Synthesis and characterization of SBA-3, SBA-15, and SBA-1 nanostructured catalytic materials J. Colloid Interf. 315 (2007): 184-190.

Pauling, L. Vitamin c and the common cold. San Francisco: W.H. Freeman, 1970.

Roberts, A.D. Natural rubber science and technology. 2nd ed. Hong Kong: Graphicraft, 1990.

Rouqerol, F., Rouqerol, J. and Sing, K. Adsorption by powders and porous solid. San Diego: Academic, 1999.

Schwartz, M.M. Composite materials. New Jersey: Prentice Hall PTR, 1996.

Suda, K. and Kornteenee, P. Natural rubber/ethylene propylene diene blends for high insulation iron crossarms. J. Appl. Polym. Sci. 92 (2004): 3401-3416.

Thai Rubber Association. World production of NR [Online]. Available from: http://www.shfe.com.cn/528/5/e27pdf [2008, December 10].

Tyndall National Institue. Hexagonal pore morphology [Online]. Available from: http://www.tyndall.ie/mai/ceramic.htm [2008, October 15].

Yang, P. The chemistry of nanostructured materials. London: World Scientific, 2003.

Yodsoontorn, P. Sorption and diffusion of organic solvent into natural rubber/polar compound blends. Master's Thesis, Department of Chemical Technology, Faculty of Science, Chulalongkorn University, 2002.

Yokoi, T., Tatsumi, T. and Yoshitake, H. Fe^{3+} coordinated to amino-functionalized MCM-41: An adsorbent for the toxic oxyanions with high capacity, resistibility to inhibiting anions, and reusability after a simple treatment, J. Colloid Interf. 274 (2004): 451-457.

APPENDICES

Appendix A

Preparation of NR solution in Toluene

(1) Calculate NR solution concentration for preparing 2.5 g_{NR} in 100 $ml_{toluene}$

From density of toluene	= 0.8669	$g\ ml^{-1}$
So, toluene 100 ml	= 86.69	g
Weight of total solution	= 86.69 + 2.5	
	= 89.19	g
Therefore, solution concentration	= (2.5/89.19) x 100	
	= 2.803	wt. %
	~ 2.8	wt. %

(2) Calculate silica material contents for filling in NR composite

In NR solution 15 g:

there is NR weight	= (2.5 x 15)/89.19	
	= 0.42	g

So, silica material content is showed in Table A-1

Table A-1 Silica Material Contents Filled in NR[a] for Preparation of NR Composite[b]

Silica material contents	
Part per hundred parts of rubber (phr[c])	Gram (g)
5	0.021
10	0.042
20	0.084
50	0.210
100	0.420
200	0.840
300	1.260

[a] NR solution 15 g that has dried NR 0.42 g.

[b] Preparation of NR Composite by slurry technique.

[c] Part per hundred part of rubber.

Appendix B

Weight Loss (TG) and Differential Weight Loss (DTG) Curve of NR Composite Studied in Research Work
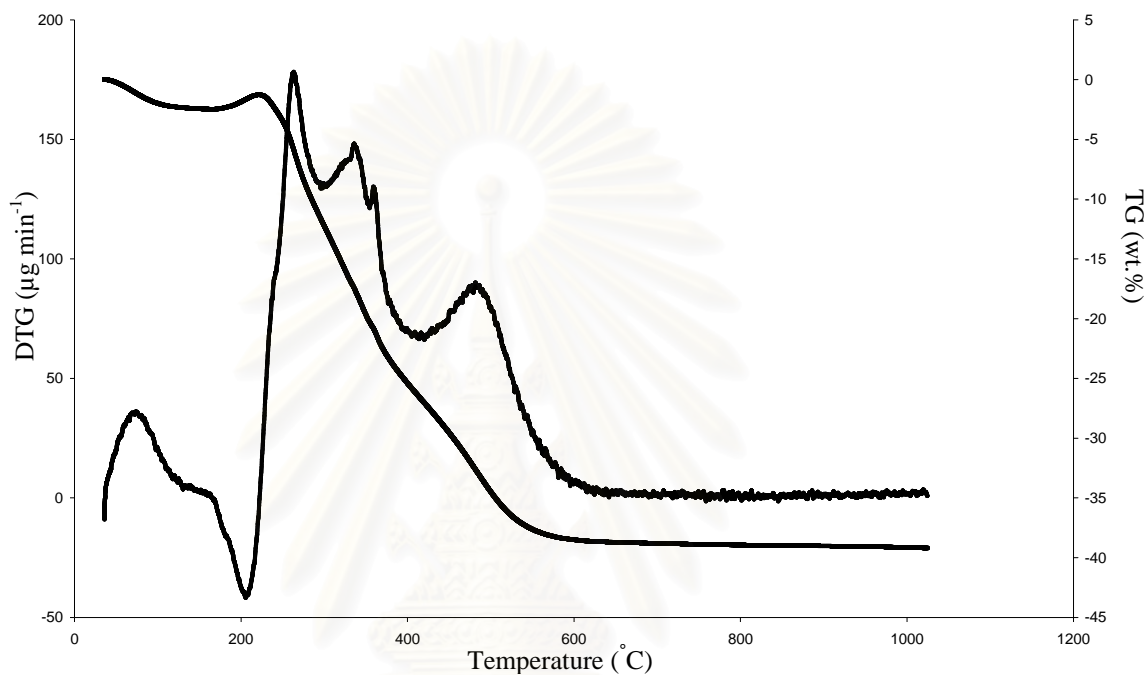
Figure B-1 Weight loss (TG) and differential weight loss (DTG) curve of
NR/Si4(200).

(1) Calculate silica materials content in NR composite prepared by slurry technique

From Figure B-1, % weight loss	= 34.08 % as NR content
Therefore, Si4 content	= 100 - 34.08
	= 65.92 %
	= 197.75 phr
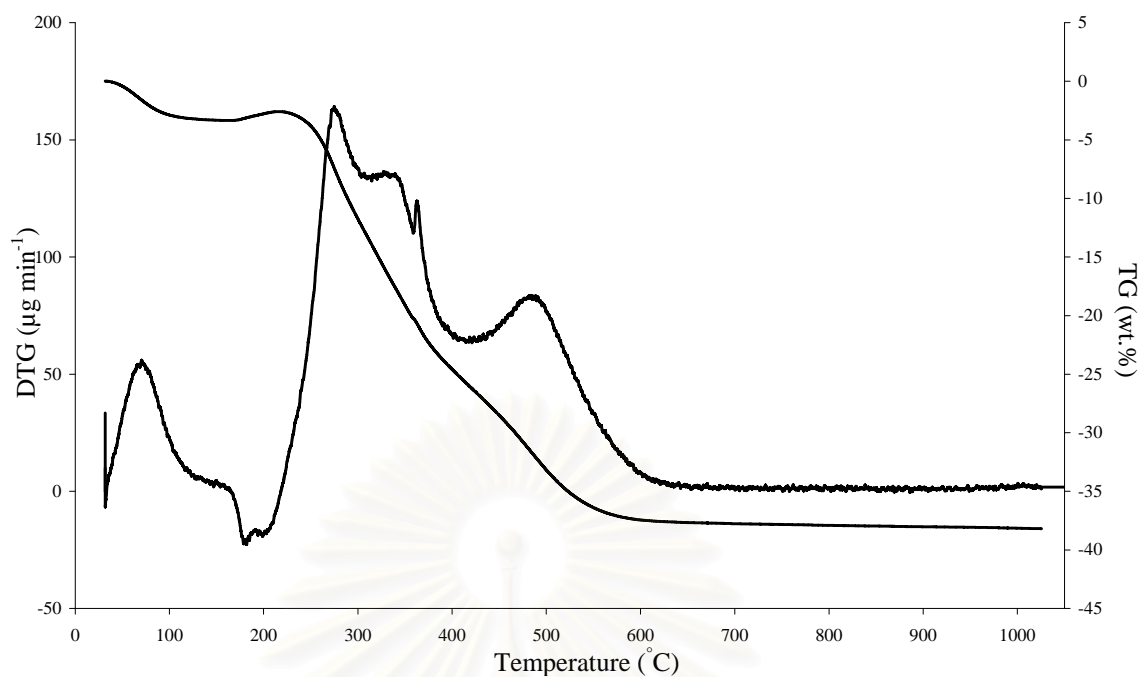
Figure B-2 Weight loss (TG) and differential weight loss (DTG) curve of NR/Si4-
S1(200).
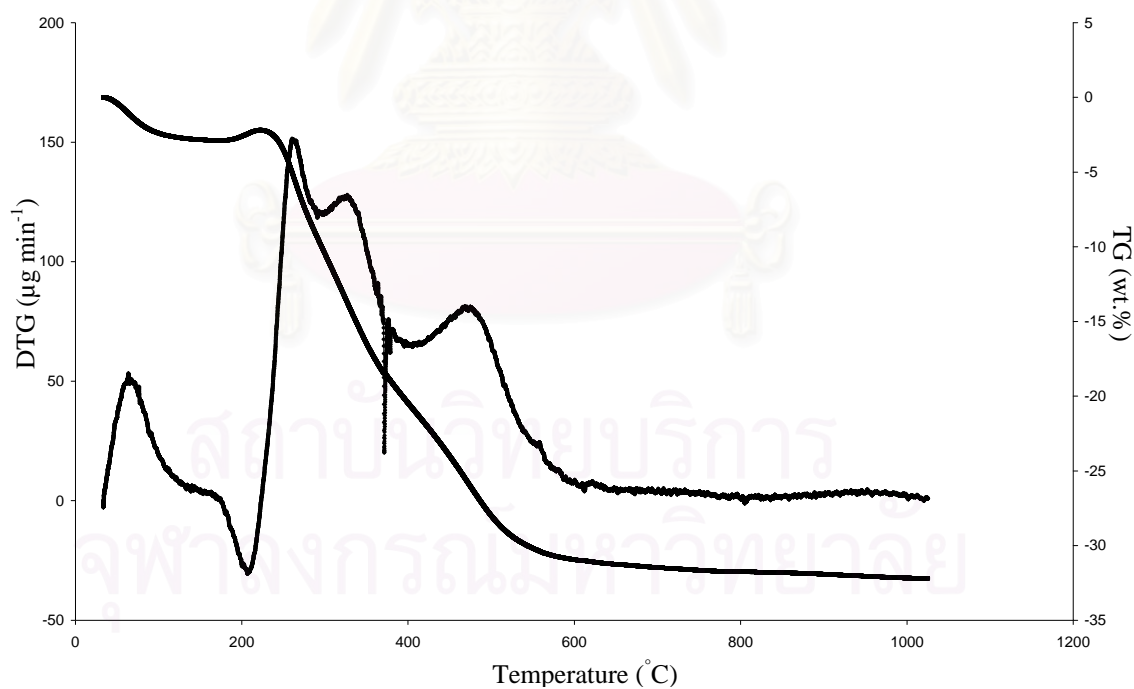
**Figure B-3** Weight loss (TG) and differential weight loss (DTG) curve of
NR/Si4(300).
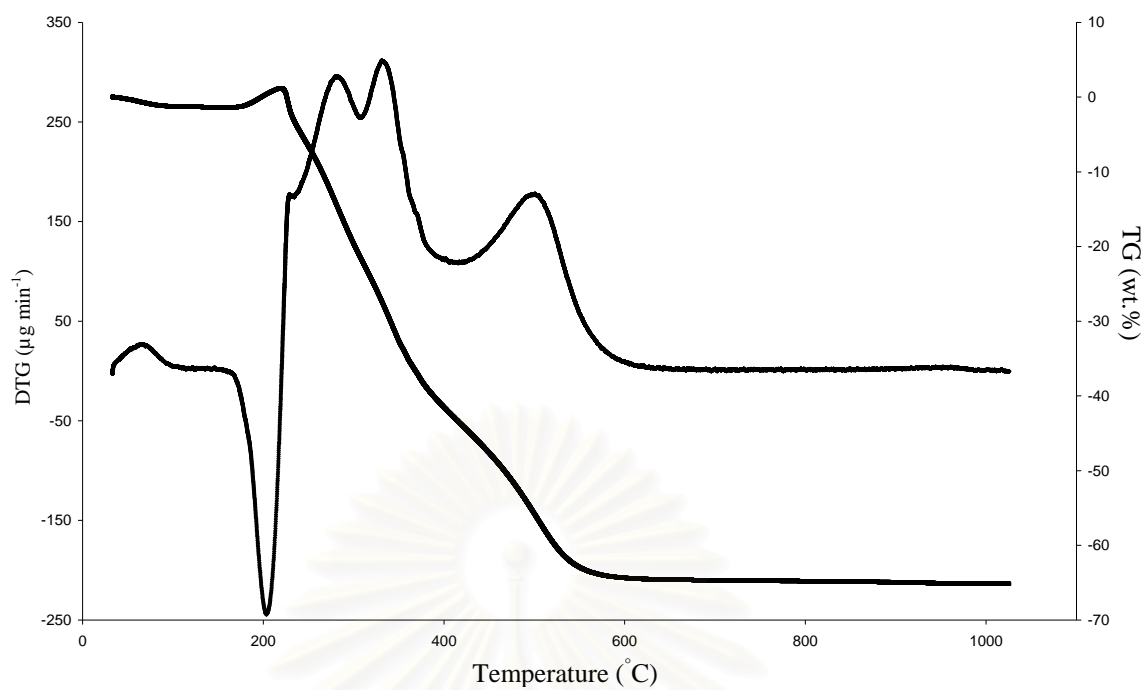
**Figure B-4** Weight loss (TG) and differential weight loss (DTG) curve of NR/MCM-41-cal(100).
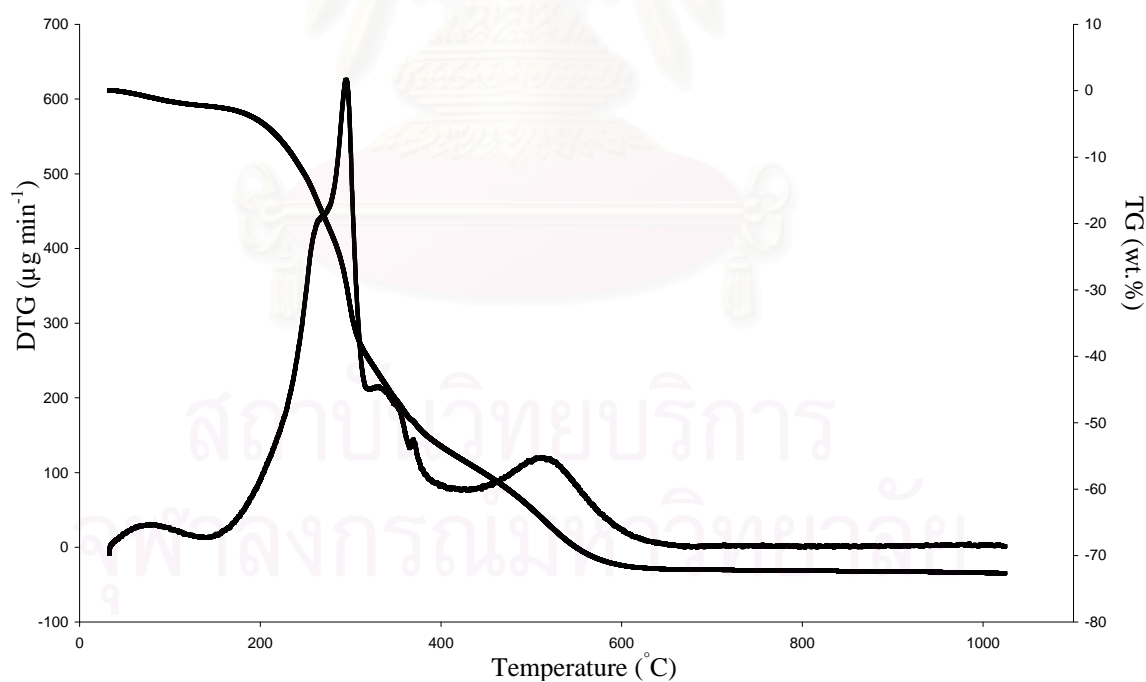
Figure B-5 Weight loss (TG) and differential weight loss (DTG) curve of NR/MCM-41-uncal.

Appendix C

Calculation of Ascorbic Acid Adsorption and Desorption

In aqueous solutions, ascorbic acid can absorb UV light at the wavelength range of 260-265 nm. For concentration range between 0.1×10^{-4} and 3.5×10^{-4} molar, Beer's law holds with sufficient exactitude to permit the use of spectrophotometric measurement for quantitative prediction of concentration. Ascorbic acid in aqueous solution can be rapidly degraded by oxidization. Therefore, sodium thiosulphate was added as ascorbic acid stabilizer in this medium over the experimental period.

The wavelength used to analyze ascorbic acid in this study was 265 nm; since, it was the λ_{max} of ascorbic acid in this medium. Table C-1 shows absorbance of each concentration of standard solution at 265 nm. Moreover a standard curve was plotted between the ascorbic acid absorbance at 265 nm and its concentration. A strange line was obtained with a coefficient determination (R^2) of 0.9984. The regression equation of this line is

$$y = 0.8789x + 0.2887 \hspace{2cm} \text{(C-1)}$$

where y is the absorbance of ascorbic acid and x is concentration of ascorbic acid solution in molar (M). This equation was then used to calculate amount of ascorbic acid desorbed from NR composite after adsorption step.

Table C-1 Calibration curve data of ascorbic acid assayed by UV/Vis -

spectrophotometer

| Standard solution no.	Concentration (molar)	Absorbance at 265 nm.
1	3.408×10^{-4}	3.2379
2	2.272×10^{-4}	2.3697
3	1.136×10^{-4}	1.2498
4	0.455×10^{-4}	0.7070
5	0.341×10^{-4}	0.6030
6	0.227×10^{-4}	0.4761
7	0.114×10^{-4}	0.3666

$y = 0.8789x + 0.2887$
$R^2 = 0.9984$
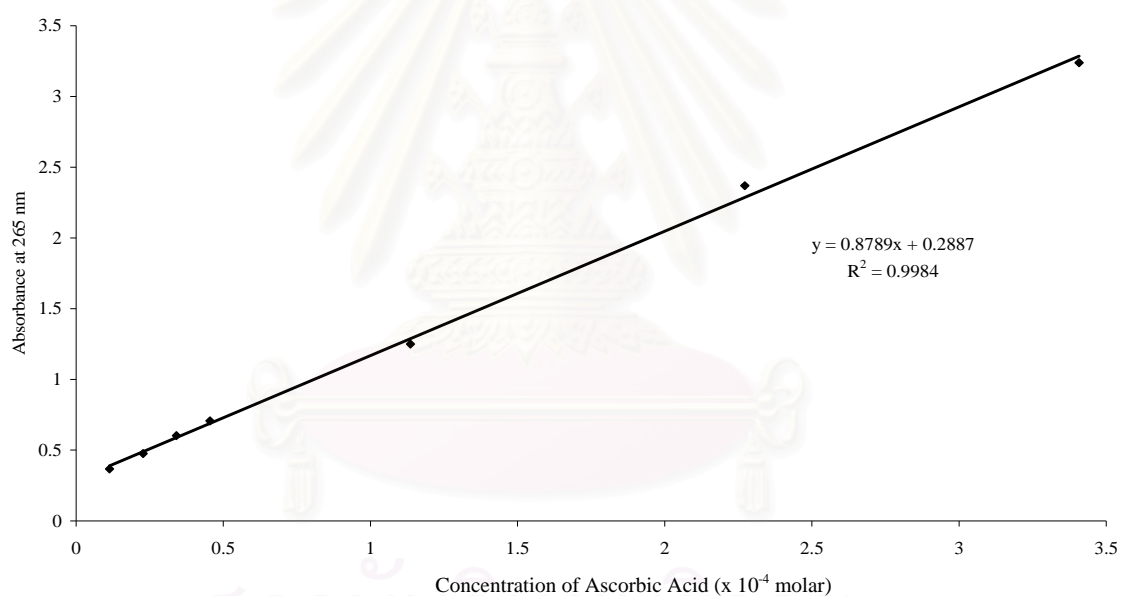
Figure C-1. Calibration curve of standard solutions of ascorbic acid in sodium

thiosulphate assayed by UV/Vis spectrophotometer ($R^2 = 0.9987$).

Table C-2 Absorbance of of Ascorbic Acid Adsorption and Desorption[a] of NR Composite at λ_{max} (265 nm)

Sample C_0[b](%w/v)	Absorbance							
	0.1	0.2	0.4	0.6	0.8	1.0	1.2	1.4
NR/Si1(100)	0.3889	0.4869	0.7049	0.9123	1.1523	1.4559	1.6132	1.8778
NR/Si1(200)	0.5556	0.6511	1.1027	1.3503	1.5503	1.9146	2.3390	2.6078
NR/Si1(300)	0.7047	0.8316	1.4071	1.7766	2.2066	2.4345	2.9081	3.2177
NR/Si4(100)	0.4215	0.6236	1.0520	1.1391	1.3391	1.4804	1.6536	1.9066
NR/Si4(200)	0.5951	0.8715	1.4027	1.6024	1.8024	2.1017	2.3964	2.6780
NR/Si4(300)	0.8059	1.0783	1.6648	1.9517	2.1917	2.6046	2.9744	3.2944
NR/MCM41(50)	0.4896	0.7068	1.0951	1.3241	1.4985	1.7109	1.8915	2.0911
NR/MCM41(80)	0.5501	0.7837	1.3732	1.7818	2.0587	2.4030	2.7012	3.0202
NR/MCM41(100)	0.6889	1.0038	1.6310	2.0906	2.4698	3.0068	3.3035	3.9910
NR/MCM41-uncal(50)	0.6908	1.0145	1.2682	1.3534	1.6003	1.8563	2.0875	2.2912
NR/MCM41-uncal(80)	0.9030	1.4197	1.6754	2.1577	2.5580	2.9475	3.0295	3.3765
NR/MCM41-uncal(100)	1.1185	2.0031	2.5093	2.8915	3.2481	3.6813	3.8959	4.1157

[a] Adsorption condition: adsorb 40 mL of 1.13 x 10^{-2}M of ascorbic acid for 15 min at ambient temperature.

Desorption condition: desorb 50 mL of 3.16 x 10^{-3}M of sodiumthiosulphate aqueous solution for 15 min at ambient temperature.

[b] Initial concentrations of ascorbic acid.

Table C-3 Amount of Ascorbic Acid Adsorption and Desorption[a] of NR Composite

Sample C_0^b(%w/v)	Amount of desorbed ascorbic acid ($\times 10^{-4}$ mole $g^{-1}_{adsorbent}$)							
	0.1	0.2	0.4	0.6	0.8	1.0	1.2	1.4
NR/Si1(100)	0.19730	0.3902	0.7638	1.1444	1.5849	2.1419	2.4306	2.9162
NR/Si1(200)	0.33744	0.4581	1.0291	1.3725	1.7336	2.2343	2.8174	3.1868
NR/Si1(300)	0.43024	0.5616	1.2236	1.6278	2.0982	2.3476	2.8657	3.2608
NR/Si4(100)	0.25191	0.6350	1.4474	1.6126	1.9919	2.2599	2.5882	2.8763
NR/Si4(200)	0.4200	0.7711	1.5089	1.7794	2.0503	2.4557	2.8550	3.2362
NR/Si4(300)	0.5827	0.8895	1.5502	1.8734	2.144	2.6089	3.0254	3.3859
NR/MCM41(50)	0.5715	1.0810	2.0852	2.677	3.1284	3.6777	4.1445	4.6608
NR/MCM41(80)	0.6197	1.1733	2.5708	3.5391	4.1955	5.0124	5.7185	6.4747
NR/MCM41(100)	0.8219	1.4686	2.7574	3.7006	4.4795	5.5824	6.1917	7.6037
NR/MCM41-uncal(50)	1.2038	2.1732	2.9327	3.1879	3.9272	4.6938	5.3858	5.9960
NR/MCM41-uncal(80)	1.4870	2.6261	3.2199	4.3398	5.2694	6.1737	6.3638	7.1698
NR/MCM41-uncal(100)	1.7815	3.4832	4.5118	5.2883	6.0127	6.8929	7.3289	7.7757

[a] Adsorption condition: adsorb 40 mL of 1.13×10^{-2}M of ascorbic acid for 15 min at ambient temperature.

Desorption condition: desorb 50 mL of 3.16×10^{-3}M of sodium thiosulphate aqueous solution for 15 min at ambient temperature.

[b] Initial concentrations of ascorbic acid.

VITA

Miss Parichart Klumratsamee was born on January 13, 1984 in Bangkok, Thailand. Her address was 1237 Sintorn village, Rangsit-pathumthani road, Tambon Bangpoon, Amphoe Mueang Pathumthani, Pathumthani 12000. She graduated with a Bachelor's degree of Engineering, majoring in Petrochemicals and Polymeric Materials, Faculty of Engineering, Silpakorn University in 2005. She has continued her study in Master's degree, majoring in Petrochemistry and Polymer Science, Faculty of Science, Chulalongkorn University, Bangkok, Thailand since 2005 and finished her study in 2008.

Presentation Experience

Oral presentation from The 17th Thailand Chemical Engineering and Applied Chemistry Conference (TICHE 17th) which organized by The Thai institute of chemical engineering and applied chemistry and Chaingmai University in the topic of "Modification of Silica Surface for Natural Rubber Composite".

Poster presentation in 3rd Mathematics & Physical Science Graduate Congress which organized by Faculty of science, University of Malaya, Kuala Lumpur, Malaysia in the topic of "Modification of Silica Surface for Natural Rubber Composite".